

# Persistent Homology in $\ell_\infty$ Metric

Gabriele Beltramo\*, Primoz Skraba

*School of Mathematical Sciences  
Queen Mary University of London, London, E1 4NS*

---

## Abstract

Proximity complexes and filtrations are a central construction in topological data analysis. Built using distance functions or more generally metrics, they are often used to infer connectivity information from point clouds. We investigate proximity complexes and filtrations built over the Chebyshev metric, also known as the maximum metric or  $\ell_\infty$  metric, rather than the classical Euclidean metric. Somewhat surprisingly, the  $\ell_\infty$  case has not been investigated thoroughly. In this paper, we examine a number of classical complexes under this metric, including the Čech, Vietoris-Rips, and Alpha complexes. We define two new families of flag complexes, which we call the Alpha flag and Minibox complexes, and prove their equivalence with Čech complexes in homological dimensions zero and one. Moreover, we provide algorithms for finding Minibox edges for two, three and higher dimensional points. Finally we run computational experiments on random points, which show that Minibox filtrations can often be used to reduce the number of simplices included in Čech filtrations, and so speed up persistent homology computations.

*Keywords:* Topological data analysis, Persistent homology, Chebyshev distance, Delaunay triangulation

---

## 1. Introduction

Topological data analysis (TDA) has been the subject of intense research over the last decade [1, 2, 3]. Persistent (co)homology is by far the most popular and studied algebraic invariant considered in TDA. Informally, this is an invariant assigned to a filtration – an increasing sequence of spaces. In our setting, a natural filtration arises from the sub-level sets of the distance to a finite sample of a space under consideration. Most commonly, the finite sample is on or near a manifold embedded in Euclidean space,  $\mathbb{R}^d$ . In the standard Euclidean setting, the Čech and the Alpha filtrations [4, 5, 6] directly capture the topology of the corresponding sub-level sets. Relatedly, the Vietoris-Rips filtration [7] provides an approximation to this topology. In particular, the corresponding filtrations in Euclidean space may be related via a sandwiching argument [8].

In this paper we study the Čech persistent homology of a finite set of points  $S$  in  $\ell_\infty$  metric space. Given  $n$  points in  $d$ -dimensional space, the Čech filtration has  $\Theta(n^{d+1})$  simplices. In the Euclidean setting, the number of simplices to be considered can be reduced by using Alpha filtrations, restricting simplices to those of the Delaunay triangulation of  $S$ . Furthermore, the Alpha filtration is known to carry the same topological information as the Čech filtration (via *homotopy equivalence*). On the other hand, we will see that the structure of  $\ell_\infty$ -Voronoi regions makes Alpha filtrations an unsuitable candidate for the computation of general Čech persistence diagrams. Moreover,  $\ell_\infty$ -Voronoi regions and their dual Delaunay triangulations have been studied primarily from a geometric standpoint and/or in low dimension [9, 10]. To overcome some of these limitations, we define two novel families of complexes: Alpha flag complexes and Minibox complexes.

---

\*This work was partially funded by the School of Mathematical Sciences at Queen Mary University of London and by the SSHRC-NFRF and DSTL/Turing Institute grant DS-015.

\*Corresponding author

*Email addresses:* g.beltramo@qmul.ac.uk (Gabriele Beltramo), p.skraba@qmul.ac.uk (Primoz Skraba)

These are both flag complexes defined on a subset of the edges of Čech complexes. Our contributions can be summarised as follows:

- Under genericity assumptions, i.e. general position, we prove that Alpha complexes are equivalent to Čech complexes for two-dimensional points, i.e. filtrations built with these complexes produce the same persistence diagrams. Moreover, we give a counterexample to this equivalence for points in higher-dimensions.
- For arbitrary dimension, we prove the equivalence of Alpha flag and Minibox complexes with Čech complexes in homological dimensions zero and one.
- We give algorithms for finding edges contained in Minibox complexes for two, three, and higher-dimensional points. In two dimensions, using a sweeping algorithm, we show a running time bound of  $O(n^2)$  (which is optimal). In three dimensions, we achieve a bound of  $O(n^2 \log(n))$  by extending the two-dimensional algorithm. In higher dimensions, using orthogonal range queries, we achieve a running time of  $O(n^2 \log^{d-1}(n))$ .
- We show that for randomly sampled points in  $\mathbb{R}^d$  the expected number of Minibox edges is proportional to  $\Theta\left(\frac{2^{d-1}}{(d-1)!} n \log^{d-1}(n)\right)$ . This is an improvement over the quadratic number of edges contained in Čech complexes, and results in smaller filtrations. Interestingly, this implies that Minibox complexes are only a polylogarithmic factor larger than  $\ell^2$ -Delaunay complexes for random points.
- We provide experimental evidence for speed ups in computation of persistence diagrams by means of Minibox filtrations.

While there is not as large a body of work on complexes in  $\ell_\infty$  metric, as there is for  $\ell_2$  metric, there are several relevant related works. In particular, approximations of  $\ell_\infty$ -Vietoris-Rips complexes are studied in [11]. Moreover, the equivalence of the different complexes in zero and one homology is related to the results of [12]. In this work offset filtrations of convex objects in two and three-dimensional space are considered. As in our case, an equivalence of filtrations is proven in homological dimensions zero and one by restricting offsets with Voronoi regions. While this result holds for general convex objects, Minibox filtrations can be used to reduce the size of  $\ell_\infty$ -Čech filtration in dimensions higher than three. We also note that our approach is similar in spirit to the preprocessing step via collapses of [13], but works directly on the geometry of the given finite point set  $S$ . Finally, we remark that all of our results hold for finite embedded points in  $\ell_1$  metric as well. As mentioned for the two-dimensional case in [9], a finite set of points can be preprocessed so as to transform  $\ell_\infty$ -balls into  $\ell_1$ -balls.

*Outline.* After introducing background information in Section 2, we study Alpha complexes and their properties in the  $\ell_\infty$  setting in Section 3. In Section 4 and 5, we introduce our two new families of flag complexes, and present the proofs of their equivalence with Čech complexes in homological dimensions zero and one. Algorithms for finding Minibox edges, and results on worst-case and expected number of Minibox edges are given in Section 6. Finally, in Section 7 we expose the results of computational experiments using Alpha flag and Minibox complexes.

## 2. Preliminaries

We introduce the relevant definitions we will use in later sections. While we aim for completeness, we point the reader to [14] for a more detailed introduction to homology and persistent homology [15, 16].

*Simplicial Complexes.* In this work we limit ourselves to simplicial complexes built on a finite set of points in  $\mathbb{R}^d$ . We denote the simplicial complex by  $K$ . We say that  $K$  is a *flag complex* if it is the clique complex of its 1-skeleton, i.e. it contains a simplex  $\sigma$  if and only if it contains all the one-dimensional faces of  $\sigma$ . We now introduce several constructions we will use. Let  $\tau$  denote a simplex in  $K$ .

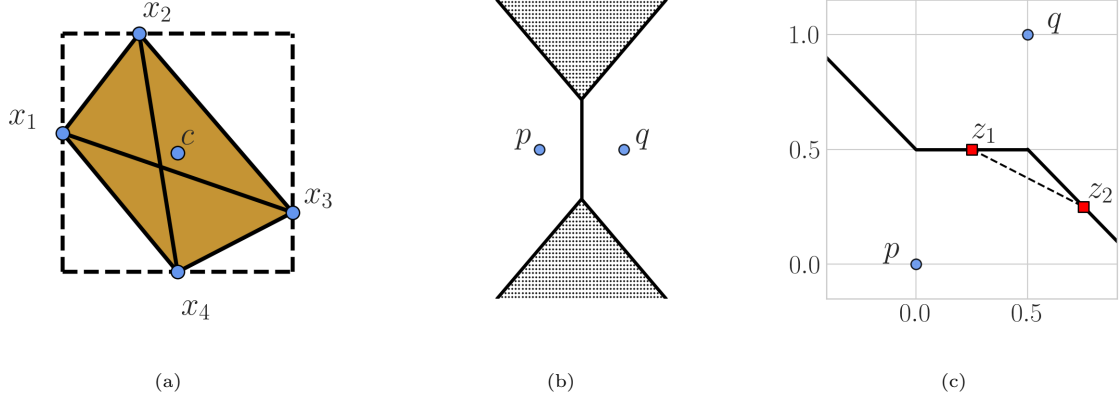


Figure 1: (a) Four points in  $\mathbb{R}^2$  whose Delaunay complex is three-dimensional. (b) Degenerate intersection of  $\ell_\infty$ -Voronoi regions. (c)  $\ell_\infty$ -Voronoi regions are not convex.

- The *nerve* of a finite collection of closed sets  $\{A_i\}_{i \in I}$  in  $\mathbb{R}^d$  is the abstract simplicial complex  $\text{Nrv}(\{A_i\}_{i \in I}) = \{\sigma \subseteq I \mid \bigcap_{i \in \sigma} A_i \neq \emptyset\}$ .
- The *star* of  $\tau$  in  $K$  is the subset of simplices of  $K$  defined by  $\text{St}(\tau) = \{\sigma \in K \mid \tau \leq \sigma\}$ .
- The *closed star*  $\text{Cl}(\text{St}(\tau))$  of  $\tau$  in  $K$  is the smallest subcomplex of  $K$  containing  $\text{St}(\tau)$ .
- The *link* of  $\tau$  in  $K$  is  $\text{Lk}(\tau) = \{\sigma \in \text{Cl}(\text{St}(\tau)) \mid \tau \cap \sigma = \emptyset\}$ .

*Balls and Boxes in  $\ell_\infty$  Metric.* Given  $p, q \in \mathbb{R}^d$ , the  $\ell_\infty$  distance, also known as maximum distance or Chebyshev distance, is defined by

$$d_\infty(p, q) = \max_{1 \leq i \leq d} \{|p_i - q_i|\}.$$

Given a point  $p \in (\mathbb{R}^d, d_\infty)$  and  $r \geq 0$ , the *open ball* of radius  $r$  and center  $p$  is  $B_r(p) = \{x \in \mathbb{R}^d \mid d_\infty(x, p) < r\}$ . We denote the *closed ball* of radius  $r$  and center  $p$  by  $\overline{B_r(p)}$ , its *boundary* by  $\partial B_r(p)$ . We have  $\varepsilon(\overline{B_r(p)}) = \overline{B_{r+\varepsilon}(p)}$ , where  $\varepsilon(A) = \{x \in \mathbb{R}^d \mid d_\infty(x, A) \leq \varepsilon\}$  is the  $\varepsilon$ -*thickening* of  $A \subseteq \mathbb{R}^d$ . Moreover, an open ball  $B_r(p)$  consists of the points  $x$  satisfying the constraints  $p_i - r < x_i$  and  $x_i < p_i + r$  for  $1 \leq i \leq d$ . Thus  $B_r(p) = \prod_{i=1}^d I_i^p$ , where  $I_i^p = (p_i - r, p_i + r)$ , which is the interior of an axis-parallel hypercube centered at  $p$ , with sides of length  $2r$ . In general we call any such Cartesian product of intervals a  $d$ -dimensional *box*. Here we recall two properties of boxes, which we often refer to in the rest of the paper. Their proofs follow directly from the facts that Cartesian products and intersections commute, and that the intersection of a finite number of intervals is either empty or an interval.

**Proposition 2.1.** *Let  $\mathcal{B}$  be a finite collection of either open or closed boxes in  $\mathbb{R}^d$ .*

- The intersection of the boxes in  $\mathcal{B}$  is equal to the Cartesian product of the intersections of intervals defining these boxes. So this intersection is either empty or a box.*
- The intersection of any subset of boxes in  $\mathcal{B}$  is non-empty if and only if all the pairwise intersections of these boxes are non-empty.*

*Voronoi diagrams and Delaunay triangulations.* These constructions have been extensively studied in computational geometry [17], primarily for Euclidean space. We refer the reader to [18] for a reference for general Voronoi diagrams and Delaunay triangulations.

**Definition 2.2.** Let  $S$  be a finite set of points in  $(\mathbb{R}^d, d_\infty)$ . The  $\ell_\infty$ -Voronoi region of a point  $p \in S$  is

$$V_p = \left\{ x \in \mathbb{R}^d \mid d_\infty(p, x) \leq d_\infty(q, x), \forall q \in S \right\}.$$

The set of  $\ell_\infty$ -Voronoi regions  $\{V_p\}_{p \in S}$  is the  $\ell_\infty$ -Voronoi diagram of  $S$ .

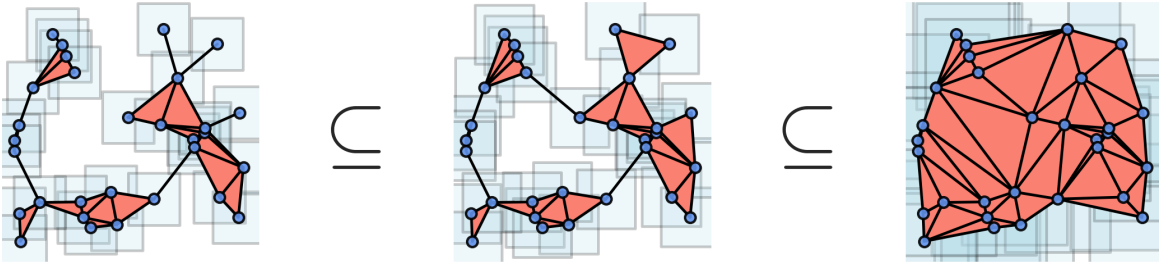


Figure 2: Alpha filtration of points in  $\mathbb{R}^2$ .

**Definition 2.3.** The *Delaunay complex* of a finite set of points  $S$  is the simplicial complex

$$K^D = \left\{ \sigma \subseteq S \mid \bigcap_{p \in \sigma} V_p \neq \emptyset \right\}.$$

The structure of intersections of Voronoi regions defined using general polyhedral norms may be degenerate. For instance, as in the Euclidean case,  $d + 2$  points in  $\mathbb{R}^d$  can have  $\ell_\infty$ -Voronoi regions with a non-empty intersection. This is illustrated by the four points in  $\mathbb{R}^2$  of Figure 1a. Moreover, without assuming any hypothesis on  $S$  the intersection of two  $\ell_\infty$ -Voronoi regions may be a  $d$ -dimensional subset of  $\mathbb{R}^d$ . For example, given any two collinear points  $p$  and  $q$  in  $\mathbb{R}^2$ ,  $V_p \cap V_q$  is the union of a line segment and two cones, the shaded areas in Figure 1b. To avoid such cases, we can impose conditions on  $S$ . In [19] the structure of Voronoi regions of polyhedral distances is studied in light of different types (weak and strong) of general position assumptions. We give different definitions of this concept in different dimensions.

**Definition 2.4.** Let  $S$  be a finite set of points in  $(\mathbb{R}^d, d_\infty)$ . We say that  $S$  is in *general position* if the distances between pairs of points in  $S$  are all distinct. Moreover, for  $d = 2$ , we require no four points in  $S$  to lie on the boundary of a square, no three points to be collinear, and no two points to have the same  $x$  or  $y$  coordinate.

We impose more conditions on points in dimension two, so that in this case  $S$  is in weak general position. This guarantees that the intersection of three Voronoi regions is either empty or a point, by [19, Corollary 3.18]. In Section 3, we make use of this result in our discussion of Alpha complexes in  $\ell_\infty$  metric space. Furthermore we give the following definition.

**Definition 2.5.** The *Delaunay triangulation* of a finite set of points  $S$  in general position in  $(\mathbb{R}^2, d_\infty)$  is the geometric realisation of the Delaunay complex  $K^D$  of  $S$ , which is the set of convex hulls of simplices of  $K^D$ .

Finally, we conclude by noting that  $\ell_\infty$ -Voronoi regions are not generally convex. To see this, we consider  $p = (0, 0)$  and  $q = (\frac{1}{2}, 1)$  and the intersection of their  $\ell_\infty$ -Voronoi regions, as in Figure 1c. These are such that  $z_1 = (\frac{1}{4}, \frac{1}{2})$ ,  $z_2 = (\frac{3}{4}, \frac{1}{4}) \in V_p, V_q$ , but the middle point on the line segment from  $z_1$  to  $z_2$  is  $\frac{z_1 + z_2}{2} = (\frac{1}{2}, \frac{3}{8})$  which belongs to  $V_p$  only. Thus  $V_q$  is not convex, so that the standard way of proving the equivalence of Alpha and Čech filtrations does not work in  $\ell_\infty$  metric. We study this problem in Section 3.

*Persistent Homology.* A *filtration* of a simplicial complex  $K$  parameterized by  $\mathcal{R}$  is a nested sequence of subcomplexes  $K_{\mathcal{R}} = \{K_{r_1} \subseteq K_{r_2} \subseteq \dots \subseteq K_{r_m}\}$ , where  $\mathcal{R} = \{r_i\}_{i=1}^m$  a finite set of monotonically increasing real values. We list three types of complexes used to define filtrations on a finite set of points  $S$ .

- The *Vietoris-Rips complex* with radius  $r$  of  $S$  is  $K_r^{VR} = \{\sigma \subseteq S \mid \max_{p, q \in S} d_\infty(p, q) \leq 2r\}$ .
- The *Čech complex* with radius  $r$  of  $S$  is  $K_r^{\check{C}} = \{\sigma \subseteq S \mid \bigcap_{p \in \sigma} \overline{B_r(p)} \neq \emptyset\}$ .
- The *Alpha complex* with radius  $r$  of  $S$  is  $K_r^A = \{\sigma \subseteq S \mid \bigcap_{p \in \sigma} (\overline{B_r(p)} \cap V_p) \neq \emptyset\}$ .

We note that for each of the complexes above we have  $K_{r_1}^\bullet \subseteq K_{r_2}^\bullet$  if  $r_1 < r_2$ . So given a monotonically increasing set of real values  $\mathcal{R}$ , we have the filtration  $K_{\mathcal{R}}^\bullet = \{K_{r_1}^\bullet \subseteq K_{r_2}^\bullet \subseteq \dots \subseteq K_{r_m}^\bullet\}$ . An example illustrating a sequence of three nested Alpha complexes of points in  $\mathbb{R}^2$  is given in Figure 2. Besides we note that from the definition of Čech and Vietoris-Rips complexes and Proposition 2.1 (ii) we have that  $K_r^{\check{C}} = K_r^{VR}$  for any  $r \in \mathbb{R}$ . Thus in  $\ell_\infty$  metric Čech complexes are flag complexes and the filtration parameter of any Čech simplex  $\sigma$  is  $\bar{r} = \frac{\max_{p,q \in \sigma} d_\infty(p,q)}{2}$ .

Given a filtration  $K_{\mathcal{R}}$ , we obtain the  $k$ -th persistence module  $M_k(K_{\mathcal{R}}) = \{H_k(K_{r_1}; \mathbb{F}) \rightarrow H_k(K_{r_2}; \mathbb{F}) \rightarrow \dots \rightarrow H_k(K_{r_m}; \mathbb{F})\}$  by applying the  $k$ -th homology functor  $H_k(-; \mathbb{F})$ , with coefficients in a field  $\mathbb{F}$ , to its elements. This admits a unique decomposition, as shown in [20], which is in bijection with a set of intervals of the form  $[r_i, r_j)$  and  $[r_i, +\infty)$ . Mapping these intervals into the points  $(r_i, r_j)$  and  $(r_i, +\infty)$ , we obtain the  $k$ -th persistence diagram  $\text{Dgm}_k(K_{\mathcal{R}})$  of the filtration  $K_{\mathcal{R}}$ . This is a multi-set of points in the extended plane  $\bar{\mathbb{R}}^2$ , where  $\bar{\mathbb{R}} = \mathbb{R} \cup \{+\infty\}$ . The bottleneck distance between two persistence diagrams  $\text{Dgm}_k(K_{\mathcal{R}}^1), \text{Dgm}_k(K_{\mathcal{R}}^2)$  is

$$d_B(\text{Dgm}_k(K_{\mathcal{R}}^1), \text{Dgm}_k(K_{\mathcal{R}}^2)) = \inf_{\eta: X \rightarrow Y} \sup_{x \in X} d_\infty(x, \eta(x)),$$

where the infimum is taken over the set of all possible bijections  $\eta : X \rightarrow Y$ ,  $X = \text{Dgm}_k(K_{\mathcal{R}}^1) \cup D$ ,  $Y = \text{Dgm}_k(K_{\mathcal{R}}^2) \cup D$ , and  $D$  is the set of diagonal points counted with infinite multiplicity. Importantly, the Stability Theorem of [21] implies that the persistence diagrams of the Čech filtrations obtained from  $S_1$  and  $S_2$  are close in bottleneck distance if the finite point sets are close in Hausdorff distance.

In practice, the persistent homology algorithm, first described in [22], takes a filtration, and outputs its persistence diagrams up to a fixed homological dimension. A substantial amount of work has been done on the computational complexity of computing persistent homology, with a large number of results [23, 24, 25, 26, 27, 28, 29] and heuristics [30, 31, 32, 33] which have greatly sped up computations in practice [34]. The standard algorithm has a complexity of  $O(m^3)$ , which can be reduced to  $O(m^\omega)$  where  $m$  is the number of simplices in the input filtrations and  $\omega$  is the matrix multiplication exponent. However, it has been observed that the majority of computation time is spent constructing the filtration. Thus smaller complexes generally result in faster computation. For instance, in the case of Čech filtrations, we have to consider  $\Theta(n^{k+2})$  simplices in order to compute their  $k$ -th persistence diagram. In Euclidean metric Čech persistent homology can be computed using Alpha filtrations, which greatly reduces the number of simplices to be considered. In the next section, we study how this translates in the  $\ell_\infty$  metric space case.

### 3. Alpha Complexes

Given a finite set of points  $S$  in Euclidean space, it is known that the filtration  $K_{\mathcal{R}}^A$  produces the same persistence diagrams of  $K_{\mathcal{R}}^{\check{C}}$ . This is proven in [15, Section 3.4] by means of the Nerve Theorem. This applies because  $K_{\mathcal{R}}^A$  is the nerve of the collection  $\{\overline{B_r(p)} \cap V_p\}_{p \in S}$ , the elements of which are all convex and closed. Together with the Persistence Equivalence Theorem of [15, Section 7.2], this proves the equivalence of  $K_{\mathcal{R}}^A$  and  $K_{\mathcal{R}}^{\check{C}}$ . Thus a way of speeding up the computation of Čech persistent homology of  $S \subseteq (\mathbb{R}^d, d_2)$  is to use its Alpha filtration. This restricts the simplices in the filtration to those in the Delaunay complex  $K^D$ , and requires computing  $K^D$  of  $S \subseteq \mathbb{R}^d$ , which contains  $O(n^{\lfloor \frac{d}{2} \rfloor})$   $d$ -simplices, and can be done efficiently only in low-dimensions [35]. In this section we investigate Alpha filtrations in  $\ell_\infty$  metric, and their possible use for the computation of Čech persistent homology.

*Alpha Filtrations in  $\mathbb{R}^2$ .* Given a two-dimensional set of points  $S$  in general position, we prove the equivalence of its Alpha and Čech filtrations for the computation of persistence diagrams. For this we make use of the following version of the Nerve Theorem.

**Theorem 3.1** (Theorem 10.7 [36]). *Let  $X$  be a triangulable space and  $\{A_i\}_{i \in I}$  a locally finite family of open subsets (or a finite family of closed subsets) such that  $X = \bigcup_{i \in I} A_i$ . If every non-empty intersection  $A_{i_1} \cap A_{i_2} \cap \dots \cap A_{i_t}$  is contractible, then  $X$  and the nerve  $\text{Nrv}(\{A_i\}_{i \in I})$  are homotopy equivalent.*

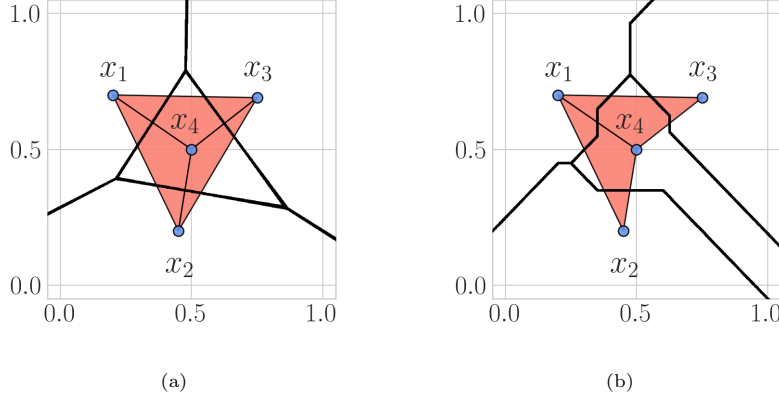


Figure 3: Voronoi diagrams and Delaunay triangulations of four points in  $\mathbb{R}^2$ , with Euclidean and  $\ell_\infty$  metric in (a) and (b) respectively.

We also need the following characterization  $\ell_\infty$ -Delaunay edges, making use of the concept of witness points. Its proof is given in Appendix A.

**Definition 3.2.** A *witness* point of  $\sigma \in K_r^A$  is a point  $z$  such that  $z \in \bigcap_{p \in \sigma} V_p \neq \emptyset$  and  $d_\infty(z, p) = \max_{p, q \in \sigma} \frac{d_\infty(p, q)}{2}$  for each  $p \in \sigma$ .

**Proposition 3.3.** Let  $S$  be a finite set of points in  $(\mathbb{R}^d, d_\infty)$ . Given a subset  $e = \{p, q\} \subseteq S$ , we define  $A_e^{\bar{r}} = \partial \overline{B_{\bar{r}}(p)} \cap \partial \overline{B_{\bar{r}}(q)}$ , where  $\bar{r} = \frac{d_\infty(p, q)}{2}$ . We have that  $A_e^{\bar{r}} = \overline{B_{\bar{r}}(p)} \cap \overline{B_{\bar{r}}(q)}$  is a non-empty box. Moreover, the set of witness points of  $e$  is  $Z_e = A_e^{\bar{r}} \setminus (\bigcup_{y \in S \setminus e} B_{\bar{r}}(y))$ , and  $e$  belongs to the  $\ell_\infty$ -Delaunay complex of  $S$  if and only if  $Z_e$  is non-empty.

**Theorem 3.4.** Let  $S$  be a finite set of points in  $(\mathbb{R}^2, d_\infty)$  in general position. The Alpha and Čech filtrations of  $S$  are equivalent, i.e. produce the same persistence diagrams.

*Proof.* Alpha complexes  $K_r^A$  are nerves of collections of closed sets  $\{\overline{B_r(p)} \cap V_p\}_{p \in S}$  for  $r \in \mathbb{R}$ . We show that any intersection of  $k$  elements in any such collection is either empty or contractible.

- $k = 2$ . Let  $p, q$  be two points of  $S$ , and  $\bar{r} = \frac{d_\infty(p, q)}{2}$ . We show that  $L = \overline{B_r(p)} \cap V_p \cap \overline{B_r(q)} \cap V_q$  is either empty or contractible. In  $\mathbb{R}^2$  we have that  $A_e^{\bar{r}} = \overline{B_{\bar{r}}(p)} \cap \overline{B_{\bar{r}}(q)}$  is a line segment of length strictly less than  $2\bar{r}$ , by our general position assumption. If this line segment is covered by  $\bigcup_{y \in S \setminus \{p, q\}} B_{\bar{r}}(y)$ , then by Proposition 3.3 we have that  $V_p \cap V_q$  is empty, so that  $L$  is empty. Moreover  $L$  is empty if  $r < \bar{r}$ , because  $\overline{B_r(p)} \cap \overline{B_r(q)}$  is. On the other hand, if  $r \geq \bar{r}$  and  $A' = A_e^{\bar{r}} \setminus \bigcup_{y \in S \setminus \{p, q\}} B_{\bar{r}}(y)$  is a non-empty line segment, and we can show that  $L$  is contractible. First we define a deformation retraction  $\phi$  of  $V_p \cap V_q$  onto  $A'$ . This is obtained by taking the Euclidean projection of  $(V_p \cap V_q) \setminus A'$  onto  $(V_p \cap V_q) \cap A'$ . This can be done because  $(V_p \cap V_q) \setminus A'$  contains a maximum of two line segments, defined by the union of points in  $\partial \overline{B_{\bar{r}+\varepsilon}(p)} \cap \partial \overline{B_{\bar{r}+\varepsilon}(q)}$  not contained in  $\bigcap_{y \in S \setminus \{p, q\}} B_{\bar{r}+\varepsilon}(y)$  for any  $\varepsilon > 0$ . For instance, considered the bisector  $V_p \cap V_q$  in Figure 1c,  $\phi$  retracts the two line segments oriented at a forty-five degree angle onto the horizontal line segment. Moreover  $\phi$  restricts to  $L$ , by the convexity of  $\overline{B_r(p)} \cap \overline{B_r(q)}$ , and the fact that this contains  $A'$  for  $r \geq \bar{r}$ . Hence  $L$  has the same homotopy type of  $A'$ , which is a line segment and so contractible.
- $k = 3$ . These intersections can either be empty or contain a single point by the general position of  $S$ .
- $k > 3$ . Any such intersection is empty, again by the general position of  $S$ .



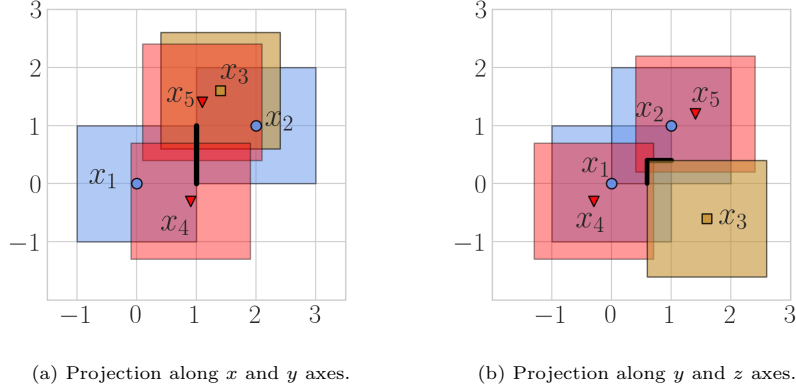


Figure 4: Five points in  $\mathbb{R}^3$  realising a counterexample to Delaunay complexes being flag complexes in dimensions higher than two.

Thus we can apply the Nerve Theorem 3.1 obtaining that  $X = \bigcup_{p \in S} (\overline{B_r(p)} \cap V_p)$  and  $K_r^A$  are homotopy equivalent for any  $r \in \mathbb{R}$ . Besides  $X = \bigcup_{p \in S} \overline{B_r(p)}$ , and by applying the Nerve Theorem to the collection  $\{\overline{B_r(p)}\}_{p \in S}$ , we have that  $X$  is homotopy equivalent to  $K_r^{\check{C}}$  as well. So  $K_r^A \simeq K_r^{\check{C}}$  for any  $r \in \mathbb{R}$ , and the desired equivalence of Alpha and Čech filtrations follows by applying the Persistence Equivalence Theorem of [15, Section 7.2].  $\square$

This is similar to the results of [12], which proves that the nerve of offsets of convex shapes is equivalent to the union of the shapes for zero and one dimensional homology in two and three dimensions. Our argument using general position implies that no higher-dimensional homology can appear in the nerve. In particular, the theorem implies that Alpha filtrations of two-dimensional points produce equivalent persistence diagrams to Čech filtrations. Hence, the above result ensures that the two-dimensional homology of Alpha complexes of  $S \subseteq \mathbb{R}^2$  is trivial, because it equals the one of the two-dimensional sets  $\bigcup_{p \in S} \overline{B_r(p)}$ . At the end of this section, we show that in general this is not the case for three-dimensional points, and so for any set of points in dimension  $d \geq 3$ .

*Alpha Filtrations in  $\mathbb{R}^2$ .* In order to construct the Alpha filtration of  $S \subseteq (\mathbb{R}^2, d_\infty)$  in general position, we need the  $\ell_\infty$ -Delaunay triangulation of  $S$ . These can be found with the  $O(n \log(n))$  plane-sweep algorithm of [9]. Moreover, it is necessary to find the radius parameter  $r_i$  of each simplex  $\sigma \in K_r^A$ , i.e. the minimum  $r_i > 0$  such that  $\bigcap_{p \in \sigma} (\overline{B_{r_i}(p)} \cap V_p) \neq \emptyset$ . For this we have the following proposition. Its proof is provided in Appendix A, and Figure 3 gives an example with four points in  $\mathbb{R}^2$  showing that the same does not hold in Euclidean metric.

**Proposition 3.5.** *Let  $S$  be a finite set of points in general position in  $(\mathbb{R}^2, d_\infty)$  and  $r \geq 0$ . Both the Delaunay complex  $K^D$  and the Alpha complex  $K_r^A$  of  $S$  are flag complexes and  $e = \{p, q\} \in K_r^A$  if and only if  $\frac{d_\infty(p, q)}{2} \leq r$ .*

Thus the radius parameter of  $\sigma \in K_r^A$  is  $\frac{\max_{p, q \in \sigma} d_\infty(p, q)}{2}$ , i.e. half the edge length of the longest edge in  $\sigma$ .

*Counterexample: The Alpha Complex is not Flag in Higher Dimensions.* We show that Proposition 3.5 does not hold for points in dimension three or higher. Given  $S = \{x_i\}_{i=1}^5 \subseteq (\mathbb{R}^3, d_\infty)$ , where  $x_1 = [0, 0, 0]$ ,  $x_2 = [2, 1, 1]$ ,  $x_3 = [1.4, 1.6, -0.6]$ ,  $x_4 = [0.9, -0.3, -0.3]$ , and  $x_5 = [1.1, 1.4, 1.2]$ , we can prove that the Alpha complex  $K_1^A$  of  $S$  is not a flag complex. In particular, we use witness points to show that  $\{x_1, x_2\}, \{x_1, x_3\}, \{x_2, x_3\} \in K_1^A$ , and  $\{x_1, x_2, x_3\} \notin K_1^A$ . One can check that:

- $(1, 0, 1)$  is a witness of  $\{x_1, x_2\}$  at distance 1 from  $x_1$  and  $x_2$ .
- $(0.8, 0.8, 0.0)$  is a witness of  $\{x_1, x_3\}$  at distance 0.8 from  $x_1$  and  $x_3$ .

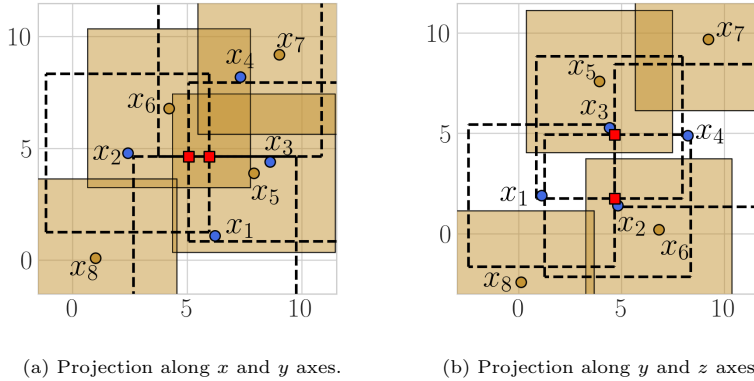


Figure 5: Counterexample to the equivalence of Alpha and Čech persistent homology in  $\ell_\infty$  metric. The two circumcenters of the tetrahedron  $\{x_1, x_2, x_3, x_4\}$  are the red square markers. The boundaries of cubes centered in the vertices of  $\{x_1, x_2, x_3, x_4\}$  are shown as dashed lines.

Table 1: Coordinates of points  $S \subseteq (\mathbb{R}^3, d_\infty)$  giving a counterexample to the equivalence of Alpha and Čech filtrations.

	x	y	z
$x_1$	6.2	1.1	1.9
$x_2$	2.4	4.8	1.4
$x_3$	8.6	4.4	5.3
$x_4$	7.3	8.2	4.9
$x_5$	7.9	3.9	7.6
$x_6$	4.2	6.8	0.2
$x_7$	9.0	9.2	9.7
$x_8$	1.0	0.1	-2.4

- $(1.5, 1.5, 0.2)$  is a witness of  $\{x_2, x_3\}$  at distance 0.8 from  $x_2$  and  $x_3$ .

Thus the pairs  $\{x_1, x_2\}$ ,  $\{x_1, x_3\}$ ,  $\{x_2, x_3\}$  are edges of the Delaunay complex  $K^D$ , and edges of  $K_1^A$  by Proposition 3.5. On the other hand  $\tau = \{x_1, x_2, x_3\}$  is not a triangle in  $K^D$ , and so does not belong to any Alpha complex. This follows from the fact that  $A_\tau^1 = \partial B_1(x_1) \cap \partial B_1(x_2) \cap \partial B_1(x_3)$  is formed by the two line segments, plotted as thickened lines in Figure 4, with endpoints  $(1, 0.6, 0)$ ,  $(1, 0.6, 0.4)$  and  $(1, 1, 0.4)$ , which are covered by  $B_1(x_4) \cup B_1(x_5)$ . The  $\varepsilon$ -thickenings of these line segments contain  $A_\tau^{1+\varepsilon}$  for any  $\varepsilon \geq 0$ , by the properties of  $\varepsilon$ -thickenings used in the proof of Proposition 3.3 in Appendix A. In turn, the  $\varepsilon$ -thickenings of the two line segments are contained in  $\varepsilon(B_1(x_4) \cup B_1(x_5)) = B_{1+\varepsilon}(x_4) \cup B_{1+\varepsilon}(x_5)$ . This implies that it does not exist a point  $z \in V_{x_1} \cap V_{x_2} \cap V_{x_3}$ , as this would require  $A_\tau^{1+\varepsilon} \cap (B_{1+\varepsilon}(x_4) \cup B_{1+\varepsilon}(x_5))$  to be non-empty for some  $\varepsilon \geq 0$ .

*Counterexample: Non-Equivalence in Higher Dimensions.* We conclude this section by providing a counterexample to the equivalence of Alpha and Čech filtrations in homological dimension two. We show a configuration of eight points  $S = \{x_i\}_{i=1}^8 \subseteq \mathbb{R}^3$  such that their Delaunay complex contains the four faces of the tetrahedron  $\{x_1, x_2, x_3, x_4\}$ , but not the tetrahedron itself. This way the Alpha complexes of  $S$  never contain  $\{x_1, x_2, x_3, x_4\}$  as a simplex, but for a big enough radius parameter they contain its the four faces. Moreover, the Delaunay complex of  $S$  also does not contain other tetrahedra that could possibly fill in the two-dimensional void created by the faces of  $\{x_1, x_2, x_3, x_4\}$ . We list the coordinates of the points giving a counterexample in Table 1, and plot them in Figure 5 by projecting along two of the three coordinate axes. These were found by randomly sampling many sets of eight points in  $\mathbb{R}^3$ , and testing whether their Alpha and Čech persistence diagrams were equal. The existence of such a counterexample can be thought of as a



consequence of the non-convexity of general  $\ell_\infty$ -Voronoi regions, even if one may hope the nerve of general Voronoi regions to be well behaved enough to prevent this from happening.

One can check that there are six tetrahedra belonging to the Delaunay complex  $K^D$  of  $S$ :  $\{x_1, x_2, x_3, x_5\}$ ,  $\{x_1, x_2, x_3, x_6\}$ ,  $\{x_1, x_2, x_4, x_5\}$ ,  $\{x_1, x_3, x_4, x_6\}$ ,  $\{x_2, x_3, x_4, x_5\}$ , and  $\{x_2, x_3, x_4, x_6\}$ . This can be done by finding the circumcenters of any four given points, and checking that the circumspheres of these (which in this case are cubes) do not contain any of the other points. It is important to note that in  $\ell_\infty$  metric four three-dimensional points might have two distinct circumcenters. For instance this is the case for  $\{x_1, x_2, x_3, x_4\}$ , the circumcenters of which are represented as red square markers in Figures 5a and 5b, having coordinates  $w_1 = (5.95, 4.65, 1.75)$  and  $w_2 = (5.05, 4.65, 4.95)$ . On the other hand, in Euclidean metric four affinely independent three-dimensional points have exactly one circumcenter. Moreover,  $w_1$  and  $w_2$  are not witnesses of  $\{x_1, x_2, x_3, x_4\}$ , because they are closer to  $x_5$  and  $x_6$  than to the vertices of this tetrahedron. Thus  $\{x_1, x_2, x_3, x_4\} \notin K^D$ . Regarding the faces of  $\{x_1, x_2, x_3, x_4\}$ , we have that:

- $(5.5, 4.2, 3.9)$  is a witness of  $\{x_1, x_2, x_3\}$  at distance 3.1 from  $x_1, x_2$ , and  $x_3$ .
- $(4.05, 4.65, 4.95)$  is a witness of  $\{x_1, x_2, x_4\}$  at distance 3.55 from  $x_1, x_2$ , and  $x_4$ .
- $(8.75, 4.65, 1.75)$  is a witness of  $\{x_1, x_3, x_4\}$  at distance 3.55 from  $x_1, x_3$ , and  $x_4$ .
- $(5.5, 5.1, 3.9)$  is a witness point of  $\{x_2, x_3, x_4\}$  at distance 3.1 from  $x_2, x_3$ , and  $x_4$ .

The tetrahedra belonging to the Delaunay complex of  $S$  (listed in the above discussion) do not create a boundary to the two-dimensional homology class created by adding  $\{x_1, x_2, x_3\}$ ,  $\{x_1, x_2, x_4\}$ ,  $\{x_1, x_3, x_4\}$ , and  $\{x_2, x_3, x_4\}$  into  $K_r^A$ , for  $r > 0$  big enough. Thus the two-dimensional persistence diagram of the Alpha filtration of  $S$  has a point at infinity, i.e. an homology class that never dies. On the other hand, the two-dimensional persistence diagrams of the Čech filtration of  $S$  cannot have such a point, because Čech complexes have trivial homology for a big enough radius.

#### 4. Alpha Flag Complexes

In the previous section we have seen that Alpha filtrations can be used to compute Čech persistence diagrams of points in  $\mathbb{R}^2$ . On the other hand, already in three dimensions there exists a set of points  $S$  having different Alpha and Čech persistence diagrams in homological dimensions two. Moreover, in Section 2 we show that in  $\ell_\infty$  metric Čech filtrations are sequences of flag complexes. In particular a simplex  $\sigma$  belongs to  $K_r^{\check{C}}$  if and only if  $\max_{p,q \in \sigma} d_\infty(p, q) \leq 2r$ . The new family of complexes we define here has the same properties.

**Definition 4.1.** The *Alpha flag complex* of  $S$  with radius  $r$  is

$$K_r^{AF} = \left\{ \sigma \subseteq S \mid \max_{p,q \in \sigma} d_\infty(p, q) \leq 2r \text{ and } \{p, q\} \in K^D \text{ for each } p, q \in \sigma \right\}$$

In this section we prove that Alpha flag and Čech persistence diagrams coincide in homological dimensions zero and one. In particular, we think of Čech filtrations as a sequence of complexes where a single edge is added when going from  $K_{r_i}^{\check{C}}$  to  $K_{r_{i+1}}^{\check{C}}$ . We prove that at each such step the zero and one-dimensional homology groups of Alpha flag and Čech complexes remain isomorphic. To deal with the problem of multiple edges having equal length, we assume that the  $\ell_\infty$  distances between pairs of points of  $S$  are all distinct, i.e.  $S$  is in general position. In case this property does not hold, the finite set of points  $S$  can be infinitesimally perturbed to obtain it. Importantly, the Stability Theorem of persistent homology, mentioned in Section 2, guarantees that the persistence diagrams of the original and perturbed points are close in bottleneck distance.

Note that to obtain the next two theorems we make use of a number of technical results, which are presented in Appendix B. Besides, we omit the field  $\mathbb{F}$ , used in Section 2, when referring to the homology of complexes, and say that a pair of points  $\{p, q\} \subseteq S$  is a non-Delaunay edge if it does not belong to the Delaunay complex of  $S$ .

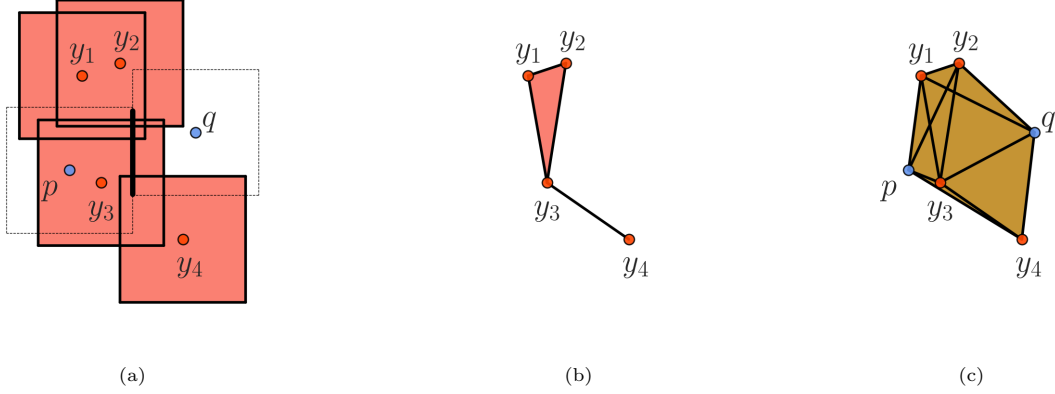


Figure 6: **(a)** Balls centered in the points of  $\bar{\mathcal{Y}} = \{y_1, y_2, y_3, y_4\}$  covering  $A_e^\bar{r}$ . **(b)**  $K_0 = \text{Nrv}(\{\overline{B_{\bar{r}}(y)}\}_{y \in \bar{\mathcal{Y}}})$ . **(c)**  $K_1$ , the union of the cones from  $K_0$  to  $p$  and  $q$ .

**Theorem 4.2.** *Let  $S$  be a finite set of points in  $(\mathbb{R}^d, d_\infty)$  in general position, and  $K_r^{\check{C}}$  the Čech complex of  $S$  with radius  $r > 0$ . If  $e = \{p, q\} \subseteq S$  is a non-Delaunay edge contained in  $K_r^{\check{C}}$ , then  $H_k(K_r^{\check{C}} \setminus \text{St}(e))$  and  $H_k(K_r^{\check{C}})$  are isomorphic in homological dimensions zero and one.*

*Proof.* We can apply the reduced Mayer-Vietoris sequence, as given in [37, Section 4.6], with  $A = \text{Cl}(\text{St}(e)) \subseteq K_r^{\check{C}}$  and  $B = K_r^{\check{C}} \setminus \text{St}(e)$ , because  $A \cap B = \text{Cl}(\text{St}(e)) \setminus \text{St}(e) \neq \emptyset$ . We obtain

$$\begin{aligned} \cdots \rightarrow \tilde{H}_k(A \cap B) \rightarrow \tilde{H}_k(A) \oplus \tilde{H}_k(B) \rightarrow \tilde{H}_k(A \cup B) \rightarrow \tilde{H}_{k-1}(A \cap B) \rightarrow \cdots \\ \downarrow \\ \cdots \rightarrow \tilde{H}_k(\text{Cl}(\text{St}(e)) \setminus \text{St}(e)) \rightarrow \tilde{H}_k(K_r^{\check{C}} \setminus \text{St}(e)) \rightarrow \tilde{H}_k(K_r^{\check{C}}) \rightarrow \tilde{H}_{k-1}(\text{Cl}(\text{St}(e)) \setminus \text{St}(e)) \rightarrow \cdots \end{aligned}$$

where  $\tilde{H}_k(A)$  cancels out, because it is trivial by definition of  $A$ . Thus showing that  $\tilde{H}_k(\text{Cl}(\text{St}(e)) \setminus \text{St}(e))$  is trivial in homological dimensions  $k$  and  $k - 1$ , implies that  $\tilde{H}_k(K_r^{\check{C}} \setminus \text{St}(e)) \rightarrow \tilde{H}_k(K_r^{\check{C}})$  is an isomorphism, from the exactness of the Mayer-Vietoris sequence above.

By definition of nerve, Proposition 2.1 (ii), and the fact that  $K_r^{\check{C}}$  is a flag complexes, it follows that  $A = \text{Cl}(\text{St}(e)) = \text{Nrv}(\{\overline{B_{\bar{r}}(y)}\}_{y \in \bar{\mathcal{Y}}})$ , where

$$\mathcal{Y} = \{y \in S \mid d_\infty(y, p) \leq 2\bar{r} \text{ and } d_\infty(y, q) \leq 2\bar{r}\}.$$

Defined  $A_e^\bar{r} = \partial \overline{B_{\bar{r}}(p)} \cap \partial \overline{B_{\bar{r}}(q)}$ , where  $\bar{r} = \frac{d_\infty(p, q)}{2} \leq r$ , we have that  $A_e^\bar{r}$  is covered by  $\bigcup_{y \in S \setminus e} B_{\bar{r}}(y)$  by Proposition 3.3. We can restrict this union of open balls to those centered in the points of

$$\bar{\mathcal{Y}} = \{y \in S \mid d_\infty(y, p) < 2\bar{r} \text{ and } d_\infty(y, q) < 2\bar{r}\} \subseteq \mathcal{Y},$$

because  $B_{\bar{r}}(y) \cap A_e^\bar{r} = \emptyset$  if  $y \notin \bar{\mathcal{Y}}$ . So  $A_e^\bar{r}$  must be covered by  $\bigcup_{y \in \bar{\mathcal{Y}}} B_{\bar{r}}(y)$  and

$$\text{Nrv}(\{\overline{B_{\bar{r}}(y)}\}_{y \in \bar{\mathcal{Y}}}) \subseteq \text{Nrv}(\{\overline{B_{\bar{r}}(y)}\}_{y \in \mathcal{Y}}) \setminus \text{St}(e) = \text{Cl}(\text{St}(e)) \setminus \text{St}(e) \subseteq K_r^{\check{C}}.$$

In Appendix B, we prove that  $\text{Nrv}(\{\overline{B_{\bar{r}}(y)}\}_{y \in \bar{\mathcal{Y}}})$  has the homotopy type of  $A_e^\bar{r}$ , and so trivial homology. The idea is that  $\text{Nrv}(\{\overline{B_{\bar{r}}(y)}\}_{y \in \bar{\mathcal{Y}}})$  has the same homotopy type of  $\bigcup_{y \in \bar{\mathcal{Y}}} \overline{B_{\bar{r}}(y)}$  by the Nerve Theorem, and that this union of balls retracts onto  $A_e^\bar{r}$ . Then, given the simplices in  $\text{Cl}(\text{St}(e)) \setminus \text{St}(e)$  and not in  $\text{Nrv}(\{\overline{B_{\bar{r}}(y)}\}_{y \in \bar{\mathcal{Y}}})$ , we prove that adding them into  $\text{Nrv}(\{\overline{B_{\bar{r}}(y)}\}_{y \in \bar{\mathcal{Y}}})$  does not alter its zero and one-dimensional homology.

Regarding zero-dimensional homology we know that  $\text{Nrv}(\{\overline{B_{\bar{r}}(y)}\}_{y \in \bar{\mathcal{Y}}})$  consists of one connected component. Also, the vertices in  $\text{Cl}(\text{St}(e)) \setminus \text{St}(e)$  not in  $\text{Nrv}(\{\overline{B_{\bar{r}}(y)}\}_{y \in \bar{\mathcal{Y}}})$ , that could potentially create a homology

class in  $\tilde{H}_0(\text{Cl}(\text{St}(e)) \setminus \text{St}(e))$ , are the points  $\mathcal{Y} \setminus \bar{\mathcal{Y}}$ . We have that  $p, q \in \mathcal{Y} \setminus \bar{\mathcal{Y}}$ , and these are fully connected to the points in  $\bar{\mathcal{Y}}$ , so do not create any connected component. Moreover, all other points in  $\mathcal{Y} \setminus \bar{\mathcal{Y}}$  are connected to both  $p$  and  $q$  by definition of  $\mathcal{Y}$ . So  $\text{Cl}(\text{St}(e)) \setminus \text{St}(e)$  cannot contain a connected component not in  $\text{Nrv}(\{\overline{B_{\bar{r}}(y)}\}_{y \in \bar{\mathcal{Y}}})$ , and  $\tilde{H}_0(\text{Cl}(\text{St}(e)) \setminus \text{St}(e))$  must be trivial.

For one-dimensional homology, we define  $K_0 = \text{Nrv}(\{\overline{B_{\bar{r}}(y)}\}_{y \in \bar{\mathcal{Y}}})$  and  $K_n = \text{Nrv}(\{\overline{B_r(y)}\}_{y \in \mathcal{Y}}) \setminus \text{St}(e)$ , and show the existence of a filtration  $K_0 \subseteq K_1 \subseteq \dots \subseteq K_n$ , such that at each step  $K_i \subseteq K_{i+1}$  no one-dimensional homology class is created. We start by defining  $K_1$  as the union of the cones from  $K_0$  to  $p$  and  $q$ . Figures 6b and 6c illustrate this step for the points in Figure 6a. So going from  $K_0$  to  $K_1$  one-dimensional homology remains trivial, because adding these cones cannot create any new 1-cycle. Then we add the points of  $y' \in \mathcal{Y} \setminus (\bar{\mathcal{Y}} \cup \{p, q\})$  into  $K_1$  one by one, obtaining a new complex  $K_{i+1}$  of the filtration above each time. Furthermore, at each such step  $K_i \subseteq K_{i+1}$ , we also add two triangles  $\{p, y', \bar{y}\}$  and  $\{q, y', \bar{y}\}$ , where  $\bar{y} \in \bar{\mathcal{Y}}$ . This can be done because  $A_e^{\bar{r}}$  is covered by  $\bigcup_{y \in \bar{\mathcal{Y}}} B_{\bar{r}}(y)$ , so that there exist  $\bar{y} \in \bar{\mathcal{Y}}$  such that  $\overline{B_r(y')} \cap \overline{B_{\bar{r}}(\bar{y})} \supseteq \overline{B_r(y')} \cap \overline{B_{\bar{r}}(\bar{y})} \neq \emptyset$ , because  $\overline{B_r(y')} \cap A_e^{\bar{r}} \neq \emptyset$ . Hence both  $\overline{B_r(p)} \cap \overline{B_r(y')} \cap \overline{B_{\bar{r}}(\bar{y})}$  and  $\overline{B_r(q)} \cap \overline{B_r(y')} \cap \overline{B_{\bar{r}}(\bar{y})}$  must be non-empty, by Proposition 2.1 (ii), so that  $\{p, y', \bar{y}\}, \{q, y', \bar{y}\} \in K_r^{\tilde{C}}$ . Thus by Proposition B.3 no one-dimensional homology class is created going from  $K_i$  to  $K_{i+1} = K_i \cup \{y'\} \cup \{p, y'\} \cup \{q, y'\} \cup \{p, y', \bar{y}\} \cup \{q, y', \bar{y}\}$ . We denote the  $K_{i+1}$  having  $\mathcal{Y}$  as its set of vertices by  $K_{n-1}$ . Finally, we add all the simplices in  $K_n \setminus K_{n-1}$  in the last filtration step. Again we can apply Proposition B.3, because for each edge  $\{y', y''\}$ , with  $y', y'' \in \mathcal{Y}$  added into  $K_n$ , there must be a triangle  $\{p, y', y''\} \in K_n$  by definition of  $\mathcal{Y}$ . Hence we can conclude that  $K_n$  has trivial reduced one-dimensional homology, i.e.  $\tilde{H}_1(\text{Cl}(\text{St}(e)) \setminus \text{St}(e))$  is trivial.

The proof follows from the exactness of the reduced Mayer-Vietoris sequence as mentioned above, and the fact that isomorphisms in reduced homology translate into isomorphisms in non-reduced homology.  $\square$

**Theorem 4.3.** *Let  $S$  be a finite set of points in  $(\mathbb{R}^d, d_\infty)$  in general position. Given  $r > 0$  and  $\varepsilon > 0$  such that  $K_{r+\varepsilon}^{\tilde{C}}$  contains exactly one edge not in  $K_r^{\tilde{C}}$ , if  $i_r^k : H_k(K_r^{AF}) \rightarrow H_k(K_r^{\tilde{C}})$  is an isomorphism, then  $i_{r+\varepsilon}^k : H_k(K_{r+\varepsilon}^{AF}) \rightarrow H_k(K_{r+\varepsilon}^{\tilde{C}})$  is also an isomorphism for  $k = 0, 1$ .*

*Proof.* Let  $e = \{p, q\} \subseteq S$  be the only edge added to  $K_r^{\tilde{C}}$  by increasing the radius parameter of  $\varepsilon > 0$ . Then either  $e$  is a Delaunay edge, so that  $e \in K_r^{AF}$  and  $e \in K_r^{\tilde{C}}$ , or  $e$  is not a Delaunay edge, so that  $e \notin K_r^{AF}$  and  $e \in K_r^{\tilde{C}}$ . We split the proof in two parts, dealing with these two cases separately.

We use the notation of Proposition 3.3, meaning that  $r < \bar{r} = \frac{d_\infty(p, q)}{2} \leq r + \varepsilon$  and  $A_e^{\bar{r}} = \overline{B_{\bar{r}}(p)} \cap \overline{B_{\bar{r}}(q)}$ . Also, as in the proof of Theorem 4.2, we define  $\bar{\mathcal{Y}} = \{y \in S \mid d_\infty(y, p) < 2\bar{r} \text{ and } d_\infty(y, q) < 2\bar{r}\}$ , so that if  $e$  is a non-Delaunay edge, then  $A_e^{\bar{r}}$  must be covered by  $\bigcup_{y \in \bar{\mathcal{Y}}} B_{\bar{r}}(y)$ .

CASE 1:  $e$  is Delaunay

For  $r > 0$  the complexes  $K_r^{AF}$  and  $K_r^{\tilde{C}}$  contain the same vertices by definition. Also, because the homomorphism induced by the inclusion of complexes  $H_0(K_r^{AF}) \rightarrow H_0(K_r^{\tilde{C}})$  is an isomorphism,  $K_r^{AF}$  and  $K_r^{\tilde{C}}$  have the same connected components. Thus after  $e$  is added in both  $K_r^{AF}$  and  $K_r^{\tilde{C}}$  either connected components do not change or the same connected component is merged in both. In the first case zero-dimensional homology remains unchanged, while in the second case the same zero-dimensional homology class is deleted in  $H_0(K_r^{AF})$  and  $H_0(K_r^{\tilde{C}})$ . In both cases  $i_r^0 : H_0(K_{r+\varepsilon}^{AF}) \rightarrow H_0(K_{r+\varepsilon}^{\tilde{C}})$  is an isomorphism induced by the inclusion  $K_{r+\varepsilon}^{AF} \subseteq K_{r+\varepsilon}^{\tilde{C}}$ .

We now look at one-dimensional homology. Adding a single edge  $e$  and the cliques it forms into  $K_r^{AF}$  and  $K_r^{\tilde{C}}$  can result in the creation or deletion of one-dimensional homology classes. We have two subcases.

1. The edge  $e$  adds nothing but itself to the Alpha flag complex  $K_r^{AF}$ ;
2. The edge  $e$  adds itself and one or more triangles to the Alpha flag complex  $K_r^{AF}$ .

SUBCASE 1.1

We start by proving that the edge  $e$  is the only simplex added into  $K_r^{\tilde{C}}$  as well. To show this, let us suppose by contradiction that increasing the radius parameter from  $r$  to  $r + \varepsilon$  results into adding  $e$  and a triangle  $\{p, q, y\}$  into  $K_r^{\tilde{C}}$ . This means  $\{p, y\}, \{q, y\} \in K_r^{\tilde{C}}$ , so that they are strictly shorter than  $\{p, q\}$  from our hypothesis on distances between pairs of points in  $S$ , i.e. general position. Given  $0 < 2\delta < 2\bar{r} - \max\{d_\infty(p, y), d_\infty(q, y)\}$ , we have  $d_\infty(p, y) < 2\bar{r} - 2\delta$  and  $d_\infty(q, y) < 2\bar{r} - 2\delta$ . Moreover  $d_\infty(p, q) = 2\bar{r}$ , so the three axis-parallel hypercubes

$\overline{B_{\bar{r}}(p)}$ ,  $\overline{B_{\bar{r}}(q)}$ , and  $\overline{B_{\bar{r}-\delta}(y)}$  have non-empty pairwise intersections. Their triple intersection is also non-empty, by Proposition 2.1 (ii), and it follows that  $A_e^{\bar{r}} \cap \overline{B_{\bar{r}}(y)} = \overline{B_{\bar{r}}(p)} \cap \overline{B_{\bar{r}}(q)} \cap \overline{B_{\bar{r}}(y)} \neq \emptyset$ . Hence the set of points  $\mathcal{Y}$  contains at least one point, and because  $e$  is a Delaunay edge, we have that  $A_e^{\bar{r}} \setminus (\bigcup_{y \in \mathcal{Y}} B_{\bar{r}}(y))$  is non-empty. Thus the closed set  $(\bigcup_{y \in \mathcal{Y}} B_{\bar{r}}(y))^c$  needs to intersect  $A_e^{\bar{r}}$ , which is a closed box. So there exist a point  $z$  of  $A_e^{\bar{r}}$  belonging to the boundary of the closure of  $\bigcup_{y \in \mathcal{Y}} B_{\bar{r}}(y)$ , otherwise  $A_e^{\bar{r}}$  would need to be disconnected, i.e.  $A_e^{\bar{r}} \cap \partial(\overline{\bigcup_{y \in \mathcal{Y}} B_{\bar{r}}(y)}) \neq \emptyset$ . Furthermore,  $z \in A_e^{\bar{r}} \cap (\bigcup_{y \in \mathcal{Y}} \partial \overline{B_{\bar{r}}(y)})$ , because  $\partial(\overline{\bigcup_{y \in \mathcal{Y}} B_{\bar{r}}(y)}) \subseteq (\bigcup_{y \in \mathcal{Y}} \partial \overline{B_{\bar{r}}(y)})$ . In conclusion  $z \in \partial \overline{B_{\bar{r}}(y')}$  for some  $y' \in \mathcal{Y}$ , and  $\{p, q, y'\}$  is a Delaunay triangle with  $z$  as a witness point, which belongs to  $K_{r+\varepsilon}^{AF}$ . This contradicts the hypothesis of Subcase 1.1, because the Alpha flag complex  $K_{r+\varepsilon}^{AF}$  cannot contain any triangles of which  $\{p, q\}$  is an edge. Thus, when increasing the radius parameter from  $r$  to  $r + \varepsilon$ , the edge  $e = \{p, q\}$  is the only simplex added in both  $K_r^{AF}$  and  $K_r^{\check{C}}$ .

In general adding a single edge to an abstract simplicial complex can result in either the deletion of a connected component or the creation of a one-dimensional homology class. The former of these two cases is dealt within the discussion of zero-dimensional homology above, and does not affect one-dimensional homology. On the other hand, if  $e$  does not merge connected components in  $K_r^{AF}$ , then it also does not merge connected components in  $K_r^{\check{C}}$ , because as already discussed zero-dimensional homology remains isomorphic. Thus both  $H_1(K_{r+\varepsilon}^{AF})$  and  $H_1(K_{r+\varepsilon}^{\check{C}})$  contain a new homology class. In this case  $i_{r+\varepsilon}^1 : H_1(K_{r+\varepsilon}^{AF}) \rightarrow H_1(K_{r+\varepsilon}^{\check{C}})$  is the isomorphism induced by the inclusion, which extends  $i_r^1 : H_1(K_r^{AF}) \rightarrow H_1(K_r^{\check{C}})$  by mapping the one-dimensional homology class created by  $e$  in  $K_{r+\varepsilon}^{AF}$  into the one created by  $e$  in  $K_{r+\varepsilon}^{\check{C}}$ .

#### SUBCASE 1.2

Adding  $e = \{p, q\}$  to both  $K_r^{AF}$  and  $K_r^{\check{C}}$  results in one or more triangles  $\{\tau_j^{\bar{r}}\}_{j \in J}$  added to the Alpha flag complex  $K_{r+\varepsilon}^{AF}$ . Moreover, by the definition of flag complex, the same triangles are added to  $K_{r+\varepsilon}^{\check{C}}$ . Also, there might be triangles  $\{\tilde{\tau}_j^{\bar{r}}\}_{j \in \tilde{J}}$  added to  $K_{r+\varepsilon}^{\check{C}}$ , which are not added to  $K_{r+\varepsilon}^{AF}$ . These  $\{\tilde{\tau}_j^{\bar{r}}\}_{j \in \tilde{J}}$  contain  $\{p, q\}$  as an edge, and at least one non-Delaunay edge among their other edges.

To begin with, we note that  $e$  does not create any one-dimensional homology class in  $K_{r+\varepsilon}^{AF}$  and  $K_{r+\varepsilon}^{\check{C}}$  by Proposition B.3. It remains to prove that a one-dimensional homology class  $[\gamma] \in H_1(K_r^{AF})$  is deleted at radius  $r + \varepsilon$  if and only if  $i_r^1([\gamma]) = [\tilde{\gamma}] \in H_1(K_r^{\check{C}})$  is also deleted.

The first direction holds because if a homology class is deleted in the Alpha flag complex, then the same formal sum of triangles is a boundary for the same homology class of the Čech complex.

For the opposite direction, let us suppose that  $[\tilde{\gamma}] \in H_1(K_r^{\check{C}})$  is deleted at radius  $r + \varepsilon$ , and that  $[\gamma]$  remains open in the Alpha flag complex with radius  $r + \varepsilon$ . We can think of adding the triangles  $\{\tau_j^{\bar{r}}\}_{j \in J}$  and  $\{\tilde{\tau}_j^{\bar{r}}\}_{j \in \tilde{J}}$  one by one in  $K_r^{\check{C}}$  in any order, obtaining a new  $\check{K}_i \subseteq K_{r+\varepsilon}^{\check{C}}$  at each step. At some point one of these must be creating a boundary deleting  $[\tilde{\gamma}]$  in  $\check{K}_i$ . If this is a triangle  $\tau_j^{\bar{r}}$  (containing Delaunay edges only), then its edges form a formal sum which is homologous to both  $[\gamma]$  and  $[\tilde{\gamma}]$ . Moreover,  $\tau_j^{\bar{r}}$  bounds this formal sums in both complexes, so that  $[\gamma] \notin H_1(K_{r+\varepsilon}^{AF})$ , which is a contradiction. On the other hand, if a non-Delaunay triangle  $\tilde{\tau}_j^{\bar{r}}$  is creating a boundary deleting  $[\tilde{\gamma}]$ , we can apply Theorem 4.2 to one of the non-Delaunay edges  $\tilde{e}$  of  $\tilde{\tau}_j^{\bar{r}}$ . We have a contradiction with the assumption of  $\tilde{\tau}_j^{\bar{r}}$  deleting  $[\tilde{\gamma}]$ , because  $K_{r+\varepsilon}^{\check{C}} \setminus \text{St}(\tilde{e})$  and  $K_{r+\varepsilon}^{\check{C}}$  need to have the same one-dimensional homology and  $\tilde{\tau}_j^{\bar{r}} \in \text{St}(\tilde{e})$ .

In conclusion the same one-dimensional homology classes are deleted in both complexes by the same triangles, and so  $i_{r+\varepsilon}^1 : H_1(K_{r+\varepsilon}^{AF}) \rightarrow H_1(K_{r+\varepsilon}^{\check{C}})$  is an isomorphism induced by the inclusion  $K_{r+\varepsilon}^{AF} \subseteq K_{r+\varepsilon}^{\check{C}}$ .

#### CASE 2: $e$ is non-Delaunay

By applying Theorem 4.2, we have that  $H_k(K_{r+\varepsilon}^{\check{C}} \setminus \text{St}(e)) \rightarrow H_k(K_{r+\varepsilon}^{\check{C}})$  is an isomorphism for  $k = 0, 1$ .

Finally, the diagram

$$\begin{array}{ccc} H_k(K_r^{AF}) & \xrightarrow{\cong} & H_k(K_{r+\varepsilon}^{\check{C}} \setminus \text{St}(e)) \\ \downarrow \cong & & \downarrow \cong \\ H_k(K_{r+\varepsilon}^{AF}) & \longrightarrow & H_k(K_{r+\varepsilon}^{\check{C}}) \end{array}$$

obtained by applying the homology functor to the inclusion maps between complexes commutes, because  $K_r^{\check{C}} = K_{r+\varepsilon}^{\check{C}} \setminus \text{St}(e)$  and  $K_r^{AF} = K_{r+\varepsilon}^{AF}$ , proving that  $H_k(K_{r+\varepsilon}^{AF}) \rightarrow H_k(K_{r+\varepsilon}^{\check{C}})$  is an isomorphism for  $k = 0, 1$ .  $\square$

**Corollary 4.4.** *Let  $S$  be a finite set of points in  $(\mathbb{R}^d, d_\infty)$  in general position. Given a finite set of monotonically increasing real-values  $\mathcal{R} = \{r_i\}_{i=1}^m$ , the Alpha flag  $K_{\mathcal{R}}^{AF}$  and Čech filtrations  $K_{\mathcal{R}}^{\check{C}}$  of  $S$  have the same persistence diagrams in homological dimensions zero and one.*

*Proof.* Given the two parameterized filtrations  $K_{r_1}^{AC} \subseteq K_{r_2}^{AC} \subseteq \dots \subseteq K_{r_m}^{AC}$  and  $K_{r_1}^{\check{C}} \subseteq K_{r_2}^{\check{C}} \subseteq \dots \subseteq K_{r_m}^{\check{C}}$ . We have that  $H_k(K_{r_i}^{AF}) \rightarrow H_k(K_{r_i}^{\check{C}})$  is an isomorphism for each  $1 \leq i \leq m$  and  $k = 0, 1$ .

- For  $r_i \leq 0$ ,  $K_{r_i}^{AF}$  and  $K_{r_i}^{\check{C}}$  are empty.
- For  $r_i > 0$ , we can think of  $K_{r_i}^{AF}$  and  $K_{r_i}^{\check{C}}$  as the result of adding one edge at a time, and the cliques these form into  $K_0^{AC}$  and  $K_0^{\check{C}}$ . Theorem 4.3 ensures that each new edge added preserves the isomorphism between the zero and one-dimensional homology groups of the Alpha flag and Čech complexes.

The proof follows by applying the Persistence Equivalence Theorem, as stated in [15, Section 7.2]  $\square$

The above result extends to generic dimension  $d$  the equivalence of zero and one-dimensional persistence diagrams proven in [12] for two and three dimensional points.

## 5. Minibox Complexes

In this section we introduce yet another family of complexes (again flag complexes), which we prove to have the same property of Alpha flag complexes, i.e. they can be used to compute the Čech persistence diagrams of  $S$  in homological dimensions zero and one. We conclude with a discussion regarding the expected number of edges these complexes can contain. In the next section, we describe algorithms for finding these edges.

**Definition 5.1.** Let  $p, q$  be two points in  $(\mathbb{R}^d, d_\infty)$ . The *minibox* of  $p$  and  $q$  is

$$\text{Mini}_{pq} = \prod_{i=1}^d (\min\{p_i, q_i\}, \max\{p_i, q_i\}),$$

that is to say the interior of the minimal bounding box of  $p$  and  $q$ .

**Proposition 5.2.** *Let  $S$  be a finite set of points in  $(\mathbb{R}^d, d_\infty)$ ,  $e = \{p, q\}$  a pair of points of  $S$ , and  $\text{Mini}_{pq}$  the minibox of  $p$  and  $q$ . If it exists  $y \in S \setminus e$  such that  $y \in \text{Mini}_{pq}$ , then  $e$  is not an edge of the  $\ell_\infty$ -Delaunay complex of  $S$ .*

*Proof.* Given  $\bar{r} = \frac{d_\infty(p, q)}{2}$ , we have  $A_e^{\bar{r}} = \overline{B_{\bar{r}}(p)} \cap \overline{B_{\bar{r}}(q)}$  by Proposition 3.3. Equivalently  $A_e^{\bar{r}} = \prod_{i=1}^d [b_i - \bar{r}, a_i + \bar{r}]$ , where  $a_i = \min\{p_i, q_i\}$  and  $b_i = \max\{p_i, q_i\}$  for each  $1 \leq i \leq d$ . Then, given  $y \in \text{Mini}_{pq}$ , it follows that  $a_i < y_i < b_i$  for each  $1 \leq i \leq d$ , implying  $y_i - \bar{r} < b_i - \bar{r}$  and  $a_i + \bar{r} < y_i + \bar{r}$ . Thus  $[b_i - \bar{r}, a_i + \bar{r}] \subset (y_i - \bar{r}, y_i + \bar{r})$  for each  $1 \leq i \leq d$ , and  $A_e^{\bar{r}} \subset B_{\bar{r}}(y)$ . The result follows applying Proposition 3.3.  $\square$

**Definition 5.3.** The *Minibox complex* of  $S$  with radius  $r$  is

$$K_r^M = \{\sigma \subseteq S \mid \max_{p, q \in \sigma} d_\infty(p, q) \leq 2r \text{ and } \text{Mini}_{pq} \cap (S \setminus \{p, q\}) = \emptyset \text{ for each } p, q \in \sigma\}$$

**Theorem 5.4.** *Let  $S$  be a finite set of points in  $(\mathbb{R}^d, d_\infty)$  in general position. Given the Alpha flag  $K_r^{AF}$  and Minibox  $K_r^M$  complexes with radius  $r$ , then  $H_k(K_r^{AF})$  and  $H_k(K_r^M)$  are isomorphic in homological dimensions zero and one.*

*Proof.* We have  $K_r^{AF} \subseteq K_r^M \subseteq K_r^{\check{C}}$ , and we know that  $H_k(K_r^{AF}) \rightarrow H_k(K_r^{\check{C}})$  is an isomorphism for  $k = 0, 1$  from the discussion in the proof of Corollary 4.4. Thus we have the following commutative diagrams, implying that  $H_k(K_r^{AF}) \rightarrow H_k(K_r^M)$  is injective for  $k = 0, 1$  and any  $r \in \mathbb{R}$ .

$$\begin{array}{ccc} K_r^{AF} & \xrightarrow{\quad} & K_r^{\check{C}} \\ & \searrow & \nearrow \\ & & K_r^M \end{array} \quad \Rightarrow \quad \begin{array}{ccc} H_k(K_r^{AF}) & \xrightarrow{\cong} & H_k(K_r^{\check{C}}) \\ & \searrow & \nearrow \\ & & H_k(K_r^M) \end{array}$$

To conclude our proof we need to show the surjectivity of this homomorphism for  $k = 0, 1$ .

For  $k = 0$ , because  $K_r^{AF}$  and  $K_r^M$  have the same set of vertices, and  $K_r^M$  might contain more edges, it follows that  $K_r^{AF}$  has the same or more connected components than  $K_r^M$ . So in homological dimension zero the homomorphism induced by the inclusion  $K_r^{AF} \subseteq K_r^M$ , must be surjective.

To prove the surjectivity of  $i_r^1 : H_1(K_r^{AF}) \rightarrow H_1(K_r^M)$ , we show that for any  $[\gamma] \in H_1(K_r^M)$  a 1-cycle  $\gamma$  representing it has to be homologous to a 1-cycle  $\gamma'$  containing Delaunay edges of length less than or equal to  $2r$ , so that  $i_r^1([\gamma']) = [\gamma]$ .

Let  $\gamma$  be a 1-cycle in  $K_r^M$  representing  $[\gamma] \in H_1(K_r^M)$ , and  $e = \{p, q\}$  the non-Delaunay edge in  $\gamma$  of maximum length. We have  $A_e^{\bar{r}} = \overline{B_{\bar{r}}(p)} \cap \overline{B_{\bar{r}}(q)}$ , where  $\bar{r} = \frac{d_\infty(p, q)}{2}$  by Proposition 3.3. Defined  $\bar{\mathcal{Y}} = \{y \in S \mid d_\infty(y, p) < 2\bar{r} \text{ and } d_\infty(y, q) < 2\bar{r}\}$ , we equivalently have  $\bar{\mathcal{Y}} = S \cap B_{2\bar{r}}(p) \cap B_{2\bar{r}}(q)$  and  $\bar{\mathcal{Y}} = S \cap \bar{r}(A_e^{\bar{r}})$ , because  $\varepsilon(A_e^{\bar{r}})$  equals  $\overline{B_{\bar{r}+\varepsilon}(p)} \cap \overline{B_{\bar{r}+\varepsilon}(q)}$  by the properties of boxes described in Appendix A. For points in  $\mathbb{R}^2$ , these sets are illustrated in Figure 7, where  $A_e^{\bar{r}}$  is represented by a thickened vertical line between  $p$  and  $q$ . Moreover, given  $c = \frac{p+q}{2}$ , we have  $\text{Mini}_{pq} \subseteq \bar{r}(c) \subseteq \bar{r}(A_e^{\bar{r}})$ , because  $c \subseteq A_e^{\bar{r}}$ , taking  $\varepsilon$ -thickenings preserves inclusions, and  $\text{Mini}_{pq}$  has sizes of length less than or equal to  $2\bar{r}$  and center  $c$ . Then, because  $e$  is not a Delaunay edge,  $A_e^{\bar{r}}$  must be covered by the union of balls centered in the points of  $S \setminus \{p, q\}$  by Proposition 3.3. Thus at least one  $y \in S \setminus \{p, q\}$  is such that  $B_{\bar{r}}(y)$  intersects  $A_e^{\bar{r}}$ , i.e.  $\bar{\mathcal{Y}} \neq \emptyset$ . Defined  $\bar{y} \in \bar{\mathcal{Y}}$  to be the point realizing

$$\min_{y \in \bar{\mathcal{Y}}} d_\infty(y, \text{Mini}_{pq}),$$

we have that  $\text{Mini}_{p\bar{y}}$  and  $\text{Mini}_{q\bar{y}}$  do not contain points in  $S \setminus \{p, q, \bar{y}\}$ , as we can show a contradiction otherwise. In particular suppose there exist either  $y' \in S \setminus \bar{\mathcal{Y}}$  or  $y'' \in \bar{\mathcal{Y}}$  belonging to one of these two miniboxes. Without loss of generality, we assume either  $y' \subseteq \text{Mini}_{p\bar{y}}$  or  $y'' \subseteq \text{Mini}_{p\bar{y}}$ . In the former case we have  $\text{Mini}_{p\bar{y}} \subseteq \bar{r}(A_e^{\bar{r}})$ , because  $p$  is on the boundary of  $\bar{r}(A_e^{\bar{r}})$  and  $\bar{y}$  in its interior. So  $y' \in \bar{r}(A_e^{\bar{r}})$ , implying that  $y' \in \bar{\mathcal{Y}}$ , which is a contradiction. In the latter case, it must be that  $d_\infty(y'', \text{Mini}_{pq}) < d_\infty(\bar{y}, \text{Mini}_{pq})$  by definition of  $\text{Mini}_{p\bar{y}}$  and  $d_\infty$ , which is in contradiction with  $\bar{y}$  being the closest point of  $\bar{\mathcal{Y}}$  to  $\text{Mini}_{pq}$ .

So there exists a vertex  $\bar{y}$  of the Minibox complex connected to  $p$  and  $q$  by the edges  $\{p, \bar{y}\}$  and  $\{q, \bar{y}\}$ . These are shorter than  $2\bar{r}$  so that  $\{p, \bar{y}\}, \{q, \bar{y}\} \subseteq K_r^M$ . Swapping  $\{p, \bar{y}\}$  and  $\{q, \bar{y}\}$  for  $e$  in  $\gamma$ , we obtain a 1-cycle homologous to  $\gamma$  with the property of having a shorter longest non-Delaunay edge. This procedure can be repeated only a finite number of times, as we have a finite number of non-Delaunay edges, and at each iteration the maximum non-Delaunay edge length in the current 1-cycle decreases. When the procedure cannot be repeated, we have a 1-cycle  $\gamma'$  in  $K_r^M$  homologous to  $\gamma$ , containing only Delaunay edges. Hence  $\gamma'$  represents a one-dimensional homology class in the Alpha flag complex which is mapped into  $[\gamma]$  by  $i_r^1 : H_1(K_r^{AF}) \rightarrow H_1(K_r^M)$ .  $\square$

**Corollary 5.5.** *Let  $S$  be a finite set of points in  $(\mathbb{R}^d, d_\infty)$  in general position. Given a finite set of monotonically increasing real-values  $\mathcal{R} = \{r_i\}_{i=1}^m$ , the Alpha flag  $K_{\mathcal{R}}^{AF}$  and Minibox filtrations  $K_{\mathcal{R}}^M$  of  $S$  have the same persistence diagrams in homological dimensions zero and one.*

*Proof.* Follows from the Persistence Equivalence Theorem of [15, Section 7.2] as for Corollary 4.4.  $\square$

*Number of Minibox Edges.* We conclude this section by studying the number of edges that a Minibox complex  $K_r^M$  can contain. We are able to show that for randomly sampled points the expected number of empty miniboxes on the points of  $S$  is proportional to  $n \cdot \text{polylog}(n)$ , where  $n$  is the number of points in  $S$ .



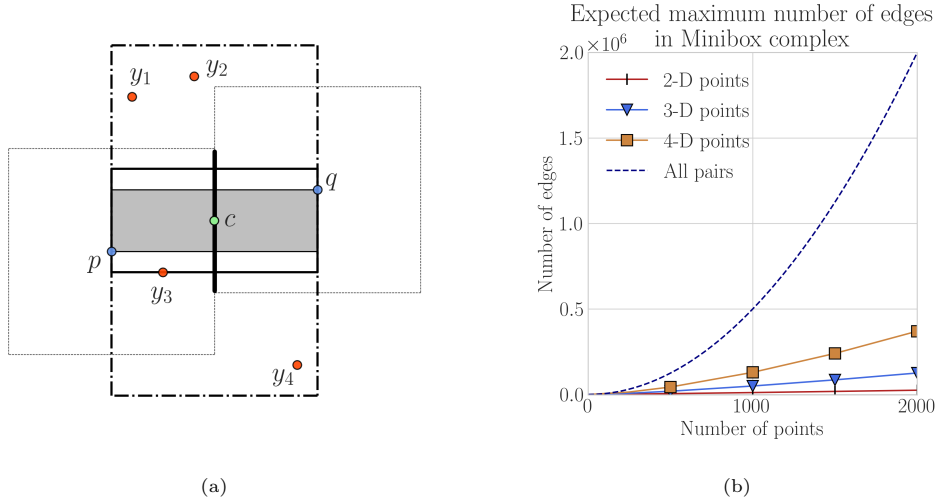


Figure 7: **(a)** The pair  $(p, q)$  is not a Delaunay edge, but is a Minibox edge.  $\text{Mini}_{pq}$  is the gray region having  $p$  and  $q$  as two vertices. The set  $\mathcal{Y}$  consists of four  $y_i$  points contained in the rectangle  $\bar{r}(A_c^r)$ , whose boundary is represented by a dash-dot line. **(b)** Expected number of Minibox edges of randomly sampled points compared to all possible edges (dashed line).

We start by noting that in the worst case a Minibox complex can contain  $O(n^2)$  edges. For example the union of  $S_1 = \{p_i = (1 - \frac{i}{n}, 1 - \frac{1}{n})\}_{i=1}^n$  and  $S_2 = \{q_j = (3 - \frac{j}{n}, 1 - \frac{j}{n})\}_{j=1}^n$  is a set of  $2n$  points in  $\mathbb{R}^2$ , on parallel line segments, such that all the miniboxes  $\text{Mini}_{p_i q_j}$  for  $1 \leq i \leq j \leq n$  do not contain any point in  $S_1 \cup S_2$ . Thus the Minibox complex of  $S_1 \cup S_2$  will contain more than  $\frac{n(n-1)}{2}$  points for a large enough radius parameter.

Next, given  $S$  to be a random points in  $\mathbb{R}^d$ , we can derive the expected number of edges contained in any maximal Minibox complex.

**Definition 5.6.** Let  $p$  and  $q$  be points in  $\mathbb{R}^d$ . We say that  $p$  *dominates*  $q$  if each of the coordinates of  $p$  is greater than the corresponding coordinate of  $q$ . Given a finite set of points  $S \subseteq \mathbb{R}^d$ , we say that  $p$  *directly dominates*  $q$  if  $p$  dominates  $q$  and there is no other point  $y \in S$  such that  $p$  dominates  $y$  and  $y$  dominates  $q$ .

**Proposition 5.7.** Let  $S$  be a finite set of uniformly distributed random points in  $(\mathbb{R}^d, d_\infty)$ . The expected number of edges contained in the maximal Minibox complex of  $S$  is  $\Theta\left(\frac{2^{d-1}}{(d-1)!} n \log^{d-1}(n)\right)$ , where  $n = |S|$ .

*Proof.* We have that if  $p$  directly dominates  $q$ , then  $\text{Mini}_{pq} \cap S = \emptyset$ . On the other hand,  $\text{Mini}_{pq} \cap S = \emptyset$  does not imply that either  $p$  directly dominates  $q$  or  $q$  directly dominates  $p$ . However, for each pair  $\{p, q\}$  there exists a sequence of a maximum of  $d$  reflections about the coordinate hyperplanes that transforms  $S$  into a set of points such that  $q$  dominates  $p$ . There are  $2^d$  possible such sequences of reflections, one for each orthant, and each produces a set of points  $S_k$  with a set of directly dominated pairs disjoint from those of the other  $S_k$ s. Moreover, if  $\{p, q\}$  is not a directly dominated pair in any  $S_k$  for  $1 \leq k \leq 2^d$ , then  $\text{Mini}_{pq} \cap S$  must be non-empty. So if the expected number of directly dominated pairs in  $S_k$  is  $m$ , then the expected number of empty miniboxes on  $S$  is  $2^{d-1} \cdot m$ , because each edge  $\{p, q\}$  is counted twice in the  $2^d$  transformed point sets  $S_k$ . In [38] it is shown that for  $n$  random points in  $\mathbb{R}^d$  the expected number of directly dominated pairs is  $\Theta\left(\frac{1}{(d-1)!} n \log^{d-1}(n)\right)$ . Thus, in dimension  $d$  there are  $\Theta\left(\frac{2^{d-1}}{(d-1)!} n \log^{d-1}(n)\right)$  pair of points  $\{p, q\}$  such that  $\text{Mini}_{pq} \cap S = \emptyset$ . The proof follows from the definition of Minibox complex.  $\square$

Figure 8b plots the expected number of minibox edges for random points in dimension  $2 \leq k \leq 4$  with  $n$  in the range  $[0, 2000]$ . This is an empirical estimate obtained by randomly sampling points in the unit hypercube and counting the number of edges found with the algorithms of the next section.



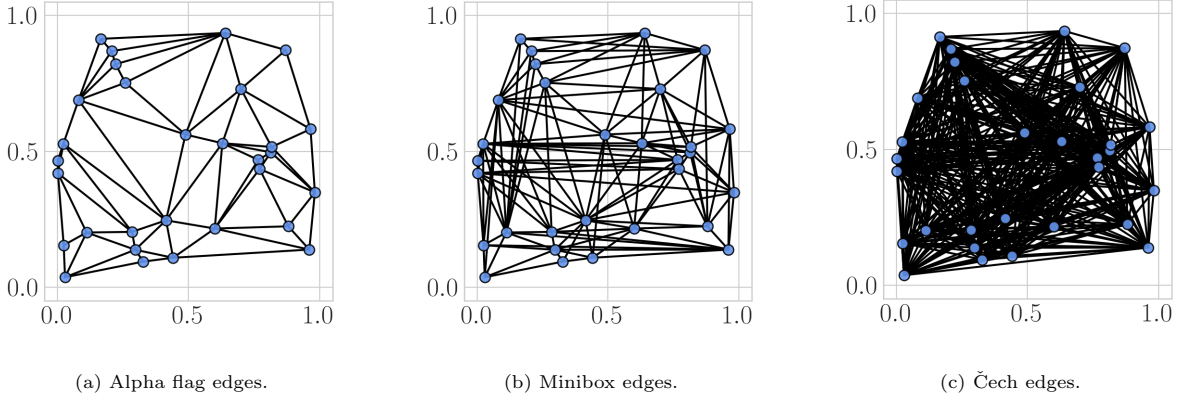


Figure 8: Comparison of Alpha flag (i.e. Delaunay), Minibox, and Čech edges of thirty random points in  $\mathbb{R}^2$ .

## 6. Algorithms

We present algorithms for finding all pairs of points  $\{p, q\} \subseteq S$  such that  $\text{Mini}_{pq} \cap S$  is empty. By definition these are all the edges a Minibox complex can contain. We study the two-dimensional, three-dimensional, and higher dimensional cases separately. For  $d = 2$  and  $d = 3$ , we present a plane-sweep and a space-sweep algorithm respectively. These maintain front data structures that can be used to efficiently determine whether  $\text{Mini}_{pq} \cap S$  is empty or not. For general dimension  $d$ , we see the problem of finding all empty miniboxes on  $S$  as of an offline orthogonal range emptiness problem with  $\frac{n(n-1)}{2}$  range queries, and reference know results on range queries.

We also provide an implementation of our algorithms in the form of the `persty` Python package, the source code of which is available at <https://github.com/gbeltramo/persty>.

*Points in two-dimensions.* We start by taking  $S$  to be a finite set of points in  $(\mathbb{R}^2, d_\infty)$ . For this case we describe a  $O(n^2)$  algorithm, whose pseudocode is given in Algorithm 1. This is worst case optimal by the discussion on the number of Minibox edges at the end of Section 5. An example of the edges contained in the maximal Minibox complex on thirty random points in  $\mathbb{R}^2$  is given in Figure 8b. This can be compared to the edges in Figures 8a and 8c showing the edges contained in the maximal Alpha flag and Čech complexes on the same points.

The algorithm works by sweeping the plane from left to right for each point  $p = (p_x, p_y)$ , starting from  $p_x$ . Then for each point  $q$  in the half plane  $(p_x, +\infty) \times (-\infty, +\infty)$  it checks whether  $(p, q)$  is a Minibox edge. This is done on line 8 of Algorithm 1. For this it uses a front, which consists of two points  $front_\uparrow$  and  $front_\downarrow$ . These are updated on line 10, and are such that  $front_\uparrow$  has a  $y$ -coordinate greater than  $p_y$ , while  $front_\downarrow$  has a  $y$ -coordinate less than or equal to  $p_y$ . Moreover defined  $X$  to be the set of points in  $S$  with  $x$ -coordinate in the range  $(p_x, q_x)$ ,  $front_\uparrow$  has a  $y$ -coordinate smaller than any other point  $x \in X$  such that  $x_y > p_y$ , and  $front_\downarrow$  has a  $y$ -coordinate larger than any other point  $x \in X$  such that  $x_y \leq p_y$ . Given  $q_y > p_y$ , by definition  $\text{Mini}_{pq}$  is non-empty if and only if there exist of point  $x \in S$  such that  $x_y > p_y$  and  $q$  dominates  $x_y$ . But such a point exists only if  $q$  dominates  $front_\uparrow$ . Thus if  $q_y > p_y$ , either  $front_\uparrow \in \text{Mini}_{pq}$  or  $\text{Mini}_{pq} \cap X = \text{Mini}_{pq} \cap S = \emptyset$ . The same applies to  $q$  with  $q_y \leq p_y$  using  $front_\downarrow$ . This is illustrated in Figure 9, where  $X = \{x_1, x_2, x_3, x_4\}$  and  $front_\uparrow = x_4$ .

The algorithm complexity is  $O(n^2)$  because we loop on all possible  $\frac{n(n-1)}{2}$  edges, and at each iteration we need  $O(1)$  operations to check whether  $\text{Mini}_{pq}$  is empty and update  $front_\uparrow, front_\downarrow$ .

*Points in three-dimensions.* For a finite set of points  $S$  in three dimensions, we present Algorithm 2, which uses a space-sweep strategy.

Given  $p, q \in S$ , we define the sweep-plane to be the  $yz$ -plane with origin  $(p_y, p_z)$ . We have that a point  $y \in \text{Mini}_{pq}$  must be such that its projection onto the sweep-plane belongs to the same quadrant as the

---

**Algorithm 1** Minibox edges of a finite set of points  $S$  in two-dimensions.

---

```

1: input: array  $points$ , the finite set of points  $S$  in  $(\mathbb{R}^2, d_\infty)$ 
2:  $edges \leftarrow$  empty list of two-tuples of integers
3: Sort  $points$  on their  $x$ -coordinate
4:  $front_\uparrow, front_\downarrow \leftarrow (p_0[0], +\infty), (p_0[0], -\infty)$ , where  $p_0 = points[0]$ 
5: for  $i = 0$  to  $|S| - 1$  do
6:   for  $j = i + 1$  to  $|S| - 1$  do
7:      $p, q \leftarrow points[i], points[j]$ 
8:     if  $Mini_{pq}$  does not contain  $front_\uparrow$  or  $front_\downarrow$  then
9:       Add  $(i, j)$  to  $edges$ 
10:      Set  $front_\uparrow = q$  if  $p[0] < q[0]$ , or  $front_\downarrow = q$  if  $p[0] \geq q[0]$ 
11:    end if
12:  end for
13: end for
14: return  $edges$ 

```

---

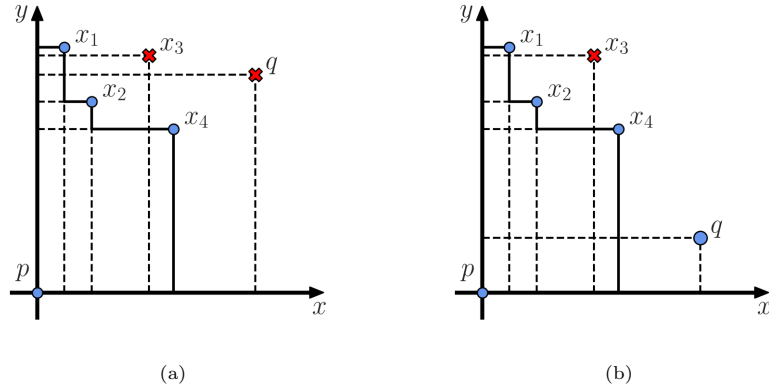


Figure 9: Illustration of the plane-sweep algorithm for Minibox edges in  $\mathbb{R}^2$ , with  $X = \{x_1, x_2, x_3, x_4\}$  and  $front_\uparrow = x_4$ . In (a)  $\{p, q\}$  is not a Minibox edge, because  $front_\uparrow \in Mini_{pq}$ . In (b)  $Mini_{pq}$  is empty, so in this case  $\{p, q\}$  is a Minibox edge.

projection of  $q$ . Hence, without loss of generality, we always assume the projection of  $q$  to belong to the first quadrant of the sweep-plane. In Algorithm 2 this reflects into the definition of  $p'$  and  $q'$  on line 8. The idea is to maintain a front data structure for each quadrant of the sweep-plane, and use it to test whether  $\{p, q\}$  is a Minibox edge or not.

At each step of the inner loop on lines 6 – 21, we have that  $\{p, q\}$  is a Minibox edge if and only if  $Mini_{p'q'}$  does not contain a point  $y'$  in the sweep-plane. Because we restrict ourselves to the first quadrant, we only need to check whether or not  $q'$  dominates any  $y'$  projected from a  $y \in S$  with  $y_x$  in the range  $(p_x, q_x)$ . To speed this up we can store the points  $y'$  as we sweep on  $(p_x, q_x)$  in a black-red tree front, sorting them on their first coordinate, and then check if  $Mini_{p'q'}$  is empty by searching among the points in this front. In particular, we only store the points  $q'$  which are adding a Minibox edge, i.e. those that do not dominate points in the front. This happens on lines 13, 16, 20 of Algorithm 2. The other points  $q''$ , dominating another point  $y'$  already in the front, are not needed. This is due to the fact that if a future  $q'$  dominates  $q''$ , then it must also dominate  $y'$ . Furthermore, it may happen for  $q'$  to be dominated by points previously stored in the front. In this case these are no longer needed, as for  $q''$  above, and we can replace them with  $q'$ , which happens on lines 13 and 16. A consequence of the way points are stored in and deleted from the red-black tree front is that these are the vertices of a staircase in the first quadrant of the sweep-plane, i.e. sorting the points along their first coordinate their second coordinates are monotonically decreasing. This disposition of

---

**Algorithm 2** Minibox edges of a finite set of points  $S$  in three-dimensions.

---

```

1: input: array  $points$ , the finite set of points  $S$  in  $(\mathbb{R}^3, d_\infty)$ 
2:  $edges \leftarrow$  empty list of two-tuples of integers
3: Sort  $points$  on their  $x$ -coordinate
4: for  $i = 0$  to  $|S| - 1$  do
5:    $fronts \leftarrow$  list of four empty red-black trees, one per quadrant
6:   for  $j = i + 1$  to  $|S| - 1$  do
7:      $p, q \leftarrow points[i], points[j]$ 
8:      $p', q' \leftarrow (0, 0), (|q[1] - p[1]|, |q[2] - p[2]|)$ 
9:      $k \leftarrow$  index such that  $(q[1], q[2])$  is in the  $k$ -th quadrant of the sweep-plane with origin  $(p[1], p[2])$ 
10:    if  $fronts[k]$  is non-empty then
11:       $y' \leftarrow$  first element to the left of  $q'$  in  $fronts[k]$  bisecting on  $q'[0]$ 
12:      if  $y'$  does not exist then
13:        Delete the points in  $fronts[k]$  that dominate  $q'$ , add  $q'$  in  $fronts[k]$ , and add  $(i, j)$  in  $edges$ 
14:      else
15:        if  $y' \notin \text{Mini}_{p'q'}$  then
16:          Delete the points in  $fronts[k]$  that dominate  $q'$ , add  $q'$  in  $fronts[k]$ , and add  $(i, j)$  in  $edges$ 
17:        end if
18:      end if
19:    else
20:      Add  $q'$  in  $fronts[k]$ , and add  $(i, j)$  in  $edges$ 
21:    end if
22:  end for
23: end for
24: return  $edges$ 

```

---

points is similar to those in the examples given for the two-dimensional case in Figure 9. The difference is that  $q'$  can be dominated by one of the points already in the front. Thus, to find  $y'$  dominated by  $q'$  in the front we can bisect on the first coordinate values of its points. This follows because if  $q'$  dominates any point in the front, then it also has to dominate the point in the front directly to its left, by the fact that the front is a staircase.

The inner loop may require to delete and add  $O(n)$  points into a red-black tree, and to bisect on the same tree  $O(n)$  times. Since either deleting, adding, or bisecting on a red-black tree requires  $O(\log(n))$  operations, we conclude that the inner loop takes a total of  $O(n \log(n))$  operations. Hence Algorithm 2 has  $O(n^2 \log(n))$  complexity.

*Higher dimensions.* For points in general dimension  $d \geq 4$ , we propose different strategies, using decreasing amount of additional storage, to test whether  $\text{Mini}_{pq} \cap S$  is empty for each pair of points in  $S$ .

For instance, high-dimensional range trees with fractional cascading [17, Section 5.6] can be used to answer orthogonal range emptiness queries in  $O(\log^{d-1}(n))$  time, at the additional cost of  $O(n \log^{d-1}(n))$  storage. By testing all pairs of points in  $S$ , we have a  $O(n^2 \log^{d-1}(n))$  algorithm. Similarly,  $kd$ -trees [17, Section 5.2] can be used to answer the same query in  $O(n^{1-\frac{1}{d}})$  time, only taking  $O(n)$  additional storage, resulting in a  $O(n^{3-\frac{1}{d}})$  algorithm for finding all the edges contained in any Minibox complex. Furthermore, we note that by the curse of dimensionality, if  $d$  becomes too big it might be faster to test each of the  $\frac{n(n-1)}{2}$  pairs of points in  $S$  via a brute force strategy, searching all points in  $S$  sequentially, which takes  $O(n)$  time. This results in a  $O(dn^3)$  total time algorithm, but does not require storing any additional data structure. The choice among these options depends on the amount of memory that can be spared for storing additional data structures. Moreover, we note that each of the above strategies could take advantage of parallel implementations using the independence of tests on each pair of points in  $S$ .

Finally, we also mention that in the Word RAM model of computation the offline orthogonal range

counting algorithm of [39] can be used to find all empty miniboxes on  $S$  in constant dimension  $d \geq 3$  in  $O(n^2 \log^{d-2+\frac{1}{d}}(n))$ . Anyway, as remarked in [39], for this algorithm to be applicable to floating-point numbers one needs to assume that the word size is at least as large as both  $\log(n)$  and the maximum size of an input number.

## 7. Computational Experiments

In this final section, we present computational experiments giving empirical evidence of the speed up obtained by using Minibox filtrations in the calculation of zero and one-dimensional Čech persistence diagrams of  $S$  in  $\ell_\infty$  metric. Moreover, we compute the persistence diagrams of Alpha flag, Minibox, and Čech filtrations obtained using randomly sampled points in  $[0, 1]^3 \subseteq (\mathbb{R}^d, d_\infty)$ . These allow us to illustrate the similarities and dissimilarities between two-dimensional diagrams of these filtrations.

We use the implementation of the persistent homology algorithm provided by the `Ripser.py` [40] Python package, in combination with the algorithms of the `persty` Python package. All computations were run on a laptop with Intel Core i7-9750H CPU with six physical cores clocked at 2.60GHz with 16GB of RAM.

*Size of Minibox filtrations.* First we study the expected size of Minibox filtrations versus the size of Čech filtrations. Our filtrations contain vertices, edges, and triangles, because we only need to compute zero and one dimensional persistence diagrams. So we have that the Čech filtration contains  $\Theta(n^3)$  simplices. Given the edges in the maximal Minibox complex of  $S$ , the clique triangles on these can be found in  $O(nk^2)$  time, where  $k$  is the maximum degree of any point in  $S$ , i.e. the maximum number of Minibox edges a point is contained in. Moreover  $O(nk^2)$  is also an upper bound on the number of possible Minibox triangles, and by Proposition 5.7 it follows that the expected value of  $k$  for a uniformly distributed finite set of random points is  $\Theta\left(\frac{2^{d-1}}{(d-1)!} \log^{d-1}(n)\right)$ . Hence, we expect the Minibox filtration of  $S$  to contain less simplices compared to the Čech filtration. We give empirical evidence of this by calculating the expected number of Minibox simplices for 500, 1000, 1500, and 2000 uniformly distributed random points, averaging over five runs. Table 2 presents our results for Minibox filtrations in two, three and four dimensions. The number of simplices contained in the Čech filtrations are listed for comparison.

Table 2: Average number of simplices contained in the Minibox and Čech filtrations for different input sizes.

	n = 500	n = 1000	n = 1500	n = 2000
Minibox 2D	$0.01 \times 10^6$	$0.03 \times 10^6$	$0.05 \times 10^6$	$0.07 \times 10^6$
Minibox 3D	$0.17 \times 10^6$	$0.50 \times 10^6$	$0.91 \times 10^6$	$1.38 \times 10^6$
Minibox 4D	$1.19 \times 10^6$	$4.50 \times 10^6$	$9.41 \times 10^6$	$15.65 \times 10^6$
Čech	$20.83 \times 10^6$	$166.67 \times 10^6$	$562.50 \times 10^6$	$1333.34 \times 10^6$

*Running Time and Memory Usage.* Next we explore the use of Minibox filtrations for the computation of Čech persistence diagrams of  $S \subseteq (\mathbb{R}^d, d_\infty)$  in homological dimensions zero and one. As already mentioned, we make use of the `Ripser.py` package, which provides a Python interface to `Ripser` [41] C++ code. In particular, we think of Minibox filtrations as of sparse filtrations, and feed into the persistent homology algorithm a precomputed sparse matrix in coordinate format. We give timing and memory usage results for points in the range [500, 32000] for Minibox filtrations, averaging over five runs. In the case of Čech filtrations we limit our experiments to a maximum of 8000 points, because of memory constraints. Moreover we consider only points in  $\mathbb{R}^2$ , as results are similar in higher dimensions.

We list our results in Tables 3, 4, 5, and 6, where columns correspond to different sizes of the input points set  $S$ , and times are given in seconds. In particular, we use Algorithm 1 for edges in Table 3, Algorithm 2

for edges in Table 4, and a brute force algorithm for edges in Table 5. We also report the average total peak memory use in megabytes.<sup>1</sup>

In all the experiments, the reduced number of simplices of Minibox filtrations results in a substantial improvement in memory usage over Čech filtrations, and in a speed up in the computation of  $Dgm_0$  and  $Dgm_1$ . This allows to increase the maximum size of inputs of the persistence algorithm, given a fixed amount of available memory. The price is having to precompute Minibox edges. We note that this computation could also take advantage of implementations parallelizing the inner loops of Algorithms 1 and 2, or the individual checks on edges of any brute force algorithm, as already mentioned in Section 6.

Table 3: Timing (seconds) and memory usage (MB) with Minibox filtrations of points in  $\mathbb{R}^2$ .

	n = 500	n = 1000	n = 2000	n = 4000	n = 8000	n = 16000	n = 32000
Edges time	0.008	0.016	0.047	0.117	0.289	0.891	2.852
Sparse matrix time	0.023	0.070	0.141	0.312	0.734	1.562	3.406
$Dgm_{0,1}$ time	0.008	0.016	0.031	0.078	0.172	0.477	1.148
Total time	0.039	0.102	0.219	0.507	1.195	2.929	7.406
Peak memory usage	2.92	5.52	11.51	25.15	53.50	112.07	246.28

Table 4: Timing (seconds) and memory usage (MB) with Minibox filtrations of points in  $\mathbb{R}^3$ .

	n = 500	n = 1000	n = 2000	n = 4000	n = 8000	n = 16000	n = 32000
Edges time	0.062	0.188	0.586	2.047	7.500	27.898	110.641
Sparse matrix time	0.117	0.281	0.742	21.871	4.609	11.289	26.555
$Dgm_{0,1}$ time	0.016	0.055	0.211	0.547	1.664	4.516	12.336
Total time	0.195	0.523	1.539	4.429	13.773	43.703	149.531
Peak memory usage	9.22	21.87	54.91	137.25	329.25	770.80	1848.01

Table 5: Timing (seconds) and memory usage (MB) with Minibox filtrations of points in  $\mathbb{R}^4$ .

	n = 500	n = 1000	n = 2000	n = 4000	n = 8000	n = 16000	n = 32000
Edges time	0.273	1.648	9.430	54.164	307.078	1657.852	8866.555
Sparse matrix time	0.258	0.727	2.055	6.250	15.680	43.516	107.773
$Dgm_{0,1}$ time	0.070	0.227	0.797	2.539	9.320	27.016	107.273
Total time	0.601	2.601	12.281	62.953	332.078	1728.383	9081.601
Peak memory usage	19.194	51.18	155.44	410.41	1122.84	2841.05	7960.18

Table 6: Timing (seconds) and memory usage (MB) with Čech filtrations of points in  $\mathbb{R}^2$ .

	n = 500	n = 1000	n = 2000	n = 4000	n = 8000
Sparse matrix time	0.656	2.758	11.047	44.789	178.727
$Dgm_{0,1}$ time	0.133	0.602	2.958	13.312	66.219
Total time	0.789	3.359	14.005	58.101	244.945
Peak memory usage	42.05	151.14	614.13	2532.38	10340.73

<sup>1</sup>In Windows this was measured using the Win32 function `GetProcessMemoryInfo()` to obtain the `PeakWorkingSetSize` memory attribute of the Python process building sparse matrices and computing persistence diagrams.

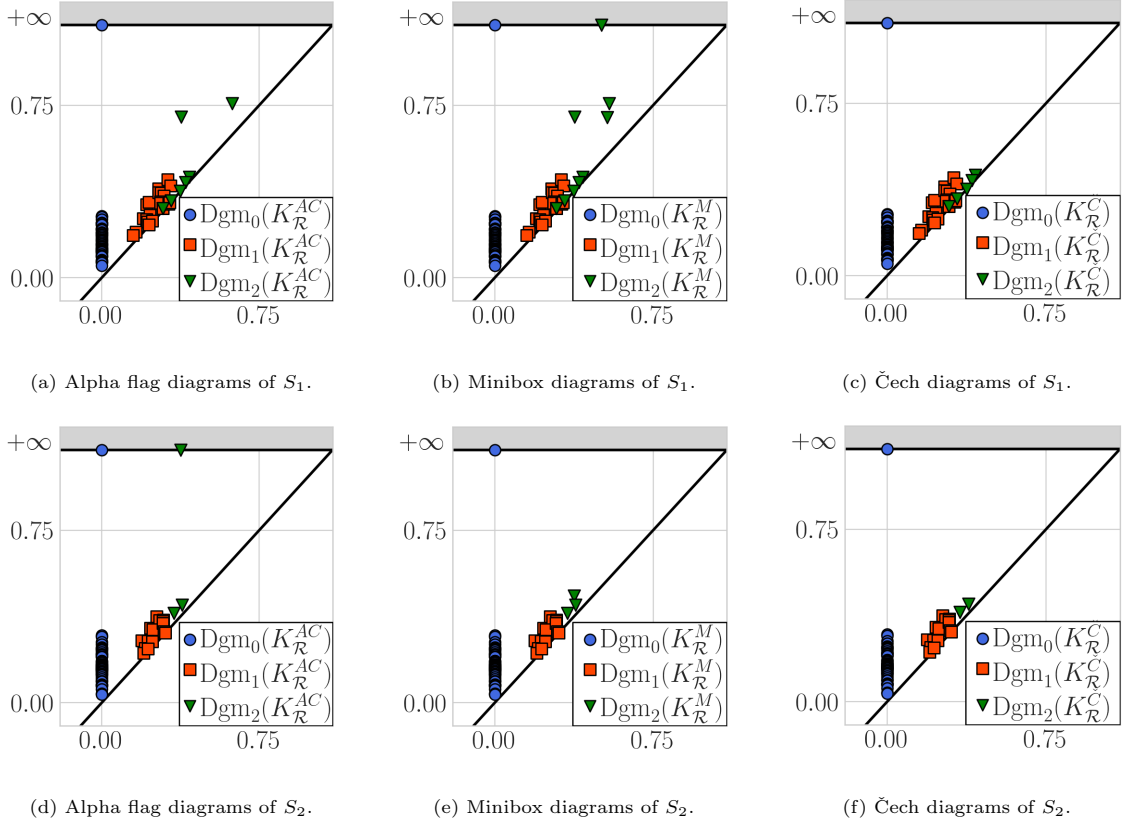


Figure 10: Persistence diagrams of finite sets of three-dimensional points in  $\ell_\infty$  metric space. Each row contains the diagrams of a different finite point set. These empirically show the equality of diagrams in dimensions zero and one, and illustrate the possible differences between diagrams of Alpha flag, Minibox, and Čech filtrations in homological dimension two.

*Differences in higher-dimensional diagrams.* We present two examples of Alpha flag, Minibox, and Čech persistence diagrams, obtained from distinct  $S_1, S_2 \subseteq (\mathbb{R}^d, d_\infty)$ . These finite point sets were obtained by randomly sampling fifty points in  $[0, 1]^3$ . The persistence diagrams were calculated with [Ripser.py](#) passing in the appropriate space matrix. For the Alpha flag case the edges belonging to the Delaunay complex of  $S_1$  and  $S_2$  were computed with a brute force strategy using the result of Proposition 3.3, i.e. checking if  $A_e^\bar{r}$  is covered by  $\bigcup_{y \in S \setminus e} B_{\bar{r}}(y)$  for each pair  $p, q \in S$ .

The first row in Figure 10 contains the diagrams of  $S_1$ . In this case  $\text{Dgm}_2(K_{\mathcal{R}}^M)$  contains a point at infinity, while  $\text{Dgm}_2(K_{\mathcal{R}}^{AF})$  does not. Furthermore, both contain additional off-diagonal points, which do not coincide. In the second row of Figure 10 we have the diagrams of  $S_2$ , and in this case it is  $\text{Dgm}_2(K_{\mathcal{R}}^{AF})$  that contains a point at infinity, while  $\text{Dgm}_2(K_{\mathcal{R}}^M)$  only has an additional off-diagonal point. This shows that it is possible to obtain Alpha flag and Minibox diagrams with off-diagonal points not contained in the corresponding Čech diagrams in homological dimensions higher than one. Furthermore,  $\text{Dgm}_2(K_{\mathcal{R}}^{AF})$  and  $\text{Dgm}_2(K_{\mathcal{R}}^M)$  are generally different, and are not one a subset of the other.

## 8. Discussion

In this paper, we prove that Alpha and Čech filtrations are equivalent for points in  $(\mathbb{R}^2, d_\infty)$ , and show a counterexample to this equivalence for higher-dimensional points. Then, we introduce two new types of proximity filtrations: the Alpha flag and Minibox filtrations. We are able to prove that both of these produce the same persistence diagrams of Čech filtrations in homological dimensions zero and one. We also describe

algorithms for finding the edges of Minibox complexes. In particular, we present an  $O(n^2)$  algorithm for two-dimensional points, a  $O(n^2 \log(n))$  algorithm for three-dimensional points, and reference [17] to obtain a  $O(n^2 \log^{d-1}(n))$  algorithm for  $d$ -dimensional points. Moreover, in the case of randomly sampled points, we prove that the expected number of these edges is proportional to  $n \cdot \text{polylog}(n)$ . Thus in many cases Minibox filtrations can be seen as a tool to drastically reduce the number of simplices to be considered in order to compute  $\ell_\infty$ -Čech persistence diagrams in homological dimensions zero and one. We also provide a number of computational experiments involving Minibox and Čech filtrations of randomly sampled points in two, three, and four-dimensional space. These show that the reduced number of simplices contained in Minibox filtrations results in a speed up of persistent homology computations, as well as in less memory being used for the same number of points. We conclude by stating two open questions, which could be the subject of future research.

- Is there a family of complexes that can be used to compute  $\ell_\infty$ -Čech persistent homology in homological dimensions higher than one?
- The geometric test for deciding whether an edge  $e$  is Delaunay is local, in the sense that it depends on an axis-parallel hyperrectangle defined by the vertices of  $e$ , by Proposition 3.3. Is it possible to produce an efficient algorithm for finding Delaunay edges in the three-dimensional case using this property? As already mentioned, the two-dimensional case is accounted for by the plane-sweep algorithm of [9].

## References

- [1] G. Carlsson, Topology and data, *Bulletin of the American Mathematical Society* 46 (2009) 255–308.
- [2] F. Chazal, B. Michel, An introduction to topological data analysis: fundamental and practical aspects for data scientists, arXiv e-prints (2017). [arXiv:1710.04019](https://arxiv.org/abs/1710.04019).
- [3] H. Edelsbrunner, J. Harer, Persistent homology—a survey, *Contemporary Mathematics* 453 (2008) 257–282.
- [4] U. Bauer, H. Edelsbrunner, The Morse theory of Čech and Delaunay filtrations, in: *Proceedings of the Thirtieth Annual Symposium on Computational Geometry*, 2014.
- [5] F. Chazal, V. De Silva, S. Oudot, Persistence stability for geometric complexes, *Geometriae Dedicata* 173 (2014) 193–214.
- [6] H. Edelsbrunner, E. P. Mücke, Three-dimensional alpha shapes, *ACM Transactions on Graphics* 13 (1994) 43–72.
- [7] L. Vietoris, Über den höheren zusammenhang kompakter räume und eine klasse von zusammenhangstreuen abbildungen, *Mathematische Annalen* 97 (1927) 454–472.
- [8] R. Ghrist, Barcodes: the persistent topology of data, *Bulletin of the American Mathematical Society* 45 (2008) 61–75.
- [9] G. M. Shute, L. L. Deneen, C. D. Thomborson, An  $O(n \log n)$  plane-sweep algorithm for  $L_1$  and  $L_\infty$  Delaunay triangulations, *Algorithmica* 6 (1991) 207–221.
- [10] J.-D. Boissonnat, M. Sharir, B. Tagansky, M. Yvinec, Voronoi diagrams in higher dimensions under certain polyhedral distance functions, *Discrete & Computational Geometry* 19 (1998) 485–519.
- [11] A. Choudhary, M. Kerber, S. Raghvendra, Improved approximate Rips filtrations with shifted integer lattices, in: *25th Annual European Symposium on Algorithms (ESA 2017)*, 2017.
- [12] D. Halperin, M. Kerber, D. Shaharabani, The offset filtration of convex objects, in: *Proceedings of the 23rd Annual European Symposium on Algorithms (ESA 2015)*, 2015.



- [13] J. Boissonnat, S. Pritam, Edge collapse and persistence of flag complexes, in: Proceedings of the 36th International Symposium on Computational Geometry, (SoCG 2020), 2020.
- [14] A. Hatcher, Algebraic Topology, Cambridge University Press, 2002.
- [15] H. Edelsbrunner, J. Harer, Computational Topology: an Introduction, American Mathematical Society, Providence, Rhode Island, 2010.
- [16] S. Y. Oudot, Persistence Theory: from Quiver Representations to Data Analysis, American Mathematical Society, Providence, Rhode Island, 2015.
- [17] M. de Berg, M. van Kreveld, M. Overmars, O. Schwarzkopf, M. Overmars, Computational Geometry: Algorithms and Applications, Springer, Berlin, Heidelberg, 2010.
- [18] F. Aurenhammer, R. Klein, D.-T. Lee, Voronoi Diagrams and Delaunay Triangulations, World Scientific Publishing Company, 2013.
- [19] F. Criado, M. Joswig, F. Santos, Tropical bisectors and Voronoi diagrams, arXiv e-prints (2019). [arXiv:1906.10950](https://arxiv.org/abs/1906.10950).
- [20] A. Zomorodian, G. Carlsson, Computing persistent homology, Discrete & Computational Geometry 33 (2005) 249–274.
- [21] D. Cohen-Steiner, H. Edelsbrunner, J. Harer, Stability of persistence diagrams, Discrete & Computational Geometry 37 (2007) 103–120.
- [22] H. Edelsbrunner, D. Letscher, A. Zomorodian, Topological persistence and simplification, Discrete & Computational Geometry 28 (2002) 511–533.
- [23] U. Bauer, M. Kerber, J. Reininghaus, Clear and compress: computing persistent homology in chunks, in: Topological Methods in Data Analysis and Visualization III, Springer International Publishing, Switzerland, 2014, pp. 103–117.
- [24] U. Bauer, M. Kerber, J. Reininghaus, Distributed computation of persistent homology, in: Proceedings of the Sixteenth Workshop on Algorithm Engineering and Experiments (ALENEX), 2014, pp. 31–38.
- [25] C. Chen, M. Kerber, Persistent homology computation with a twist, in: Proceedings of the 27th European Workshop on Computational Geometry, 2011.
- [26] V. De Silva, D. Morozov, M. Vejdemo-Johansson, Dualities in persistent (co)homology, Inverse Problems 27 (2011) 124003.
- [27] N. Milosavljević, D. Morozov, P. Skraba, Zigzag persistent homology in matrix multiplication time, in: Proceedings of the Twenty-Seventh Annual Symposium on Computational Geometry, 2011.
- [28] K. Mischaikow, V. Nanda, Morse theory for filtrations and efficient computation of persistent homology, Discrete & Computational Geometry 50 (2013) 330–353.
- [29] H. Wagner, C. Chen, E. Vućini, Efficient computation of persistent homology for cubical data, in: Topological Methods in Data Analysis and Visualization II, Springer-Verlag, Berlin, Heidelberg, 2012, pp. 91–106.
- [30] M. B. Botnan, G. Spreemann, Approximating persistent homology in Euclidean space through collapses, Applicable Algebra in Engineering, Communication and Computing 26 (2015) 73–101.
- [31] C. Chen, M. Kerber, An output-sensitive algorithm for persistent homology, Computational Geometry 46 (2013) 435–447.

- [32] M. Kerber, R. Sharathkumar, Approximate Čech complex in low and high dimensions, in: Proceedings of the 24th International Symposium on Algorithms and Computation, 2013.
- [33] D. R. Sheehy, Linear-size approximations to the Vietoris–Rips filtration, *Discrete & Computational Geometry* 49 (2013) 778–796.
- [34] N. Otter, M. A. Porter, U. Tillmann, P. Grindrod, H. A. Harrington, A roadmap for the computation of persistent homology, *EPJ Data Science* 6 (2017) 17.
- [35] S. Hornus, J.-D. Boissonnat, An efficient implementation of Delaunay triangulations in medium dimensions, Research Report, INRIA, 2008. URL: <https://hal.inria.fr/inria-00343188>.
- [36] R. L. Graham, M. Grötschel, L. Lovász, *Handbook of Combinatorics, Volume II*, Elsevier, 1995.
- [37] E. H. Spanier, *Algebraic Topology*, Springer-Verlag, New York, 2012.
- [38] R. Klein, Direct dominance of points, *International Journal of Computer Mathematics* 19 (1986) 225–244.
- [39] T. M. Chan, M. Pătraşcu, Counting inversions, offline orthogonal range counting, and related problems, in: Proceedings of the Twenty-First Annual ACM-SIAM Symposium on Discrete Algorithms, 2010.
- [40] C. Tralie, N. Saul, R. Bar-On, Ripser.py: A lean persistent homology library for Python, *The Journal of Open Source Software* 3 (2018) 925. URL: <https://doi.org/10.21105/joss.00925>.
- [41] U. Bauer, Ripser: efficient computation of vietoris-rips persistence barcodes, arXiv e-prints (2019). [arXiv:1908.02518](https://arxiv.org/abs/1908.02518).

## A. $\ell_\infty$ -Delaunay Edges

In this section we provide a proof of the characterization of  $\ell_\infty$ -Delaunay edges in terms of witness points. Using this, we also show that Delaunay and Alpha complexes of two-dimensional points in  $\ell_\infty$  metric are flag complexes.

We recall that we define a box to be an axis-parallel hyperrectangle, i.e. the Cartesian product of  $d$  intervals in  $\mathbb{R}^d$ . As discussed in Section 2, we have that  $\ell_\infty$ -balls are boxes with sizes of length  $2r$  and that a finite set of  $\ell_\infty$ -balls has a non-empty intersection if and only if all pairwise intersections of  $\ell_\infty$ -balls are non-empty. Moreover, we use the notion of general position defined in the main paper. So the intersections of  $\ell_\infty$ -Voronoi regions of points in  $\mathbb{R}^2$  are never degenerate. We start by showing some properties of  $\varepsilon$ -thickenings, which we use throughout this section.

**Proposition A.1.** (i) *Let  $I_1, I_2 \subseteq \mathbb{R}$  be two non-empty closed intervals. If  $I_1 \cap I_2 \neq \emptyset$ , then  $\varepsilon(I_1 \cap I_2) = \varepsilon(I_1) \cap \varepsilon(I_2)$ .*

(ii) *Let  $B_1, B_2 \subseteq \mathbb{R}$  be two non-empty boxes. If  $B_1 \cap B_2 \neq \emptyset$ , then  $\varepsilon(B_1 \cap B_2) = \varepsilon(B_1) \cap \varepsilon(B_2)$ .*

(iii) *Taking  $\varepsilon$ -thickenings preserves inclusions.*

(iv) *Let  $\mathcal{A} = \{A\}_{i \in I}$  be a finite collection of sets. The  $\varepsilon$ -thickening of the union of sets in  $\mathcal{A}$  is equal to the union of the  $\varepsilon$ -thickenings of sets in  $\mathcal{A}$ .*

*Proof.* (i) We have  $I_1 = [a_1, b_1]$  and  $I_2 = [a_2, b_2]$ , with  $I_1 \cap I_2 \neq \emptyset$ . So either one of the two intervals is contained in the other or they share a common subinterval. In the first case, we can suppose without loss of generality  $I_1 \subseteq I_2$ . Then  $\varepsilon(I_1 \cap I_2) = \varepsilon(I_1) = [a_1 - \varepsilon, b_1 + \varepsilon] = [a_1 - \varepsilon, b_1 + \varepsilon] \cap [a_2 - \varepsilon, b_2 + \varepsilon] = \varepsilon(I_1) \cap \varepsilon(I_2)$ . In the latter case, we can assume without loss of generality that  $I_1 \cap I_2 = [a_2, b_1]$ , and we have  $\varepsilon(I_1 \cap I_2) = [a_2 - \varepsilon, b_1 + \varepsilon] = [a_1 - \varepsilon, b_1 + \varepsilon] \cap [a_2 - \varepsilon, b_2 + \varepsilon] = \varepsilon(I_1) \cap \varepsilon(I_2)$ .

(ii) Follows from property (i) and the definition of box.

(iii) We consider  $A, B \subseteq \mathbb{R}^d$  such that  $A \subseteq B$ . Given any  $x \in \varepsilon(A) \setminus A$ , by the definition of  $\varepsilon$ -thickening there exists  $a \in A$  such that  $d_\infty(x, a) \leq \varepsilon$ . We have that  $x \in \varepsilon(B)$ , because  $a \in B$  and  $d_\infty(x, a) \leq \varepsilon$ . So  $\varepsilon(A) \setminus A \subseteq \varepsilon(B)$ , and because  $A \subseteq \varepsilon(B)$  it follows that  $\varepsilon(A) \subseteq \varepsilon(B)$ .

(iv) For any set  $A \subseteq \mathbb{R}^d$ , we have  $\varepsilon(A) = \bigcup_{x \in A} \overline{B_\varepsilon(x)}$ . Thus

$$\varepsilon\left(\bigcup_{i \in I} A_i\right) = \bigcup_{x \in \bigcup_{i \in I} A_i} \overline{B_\varepsilon(x)} = \bigcup_{i \in I} \bigcup_{x \in A_i} \overline{B_\varepsilon(x)} = \bigcup_{i \in I} \varepsilon(A_i)$$

□

We now give the proof of the main result of this section, and state the definition of witness point as provided in the main paper for completeness.

**Definition A.2.** A *witness* point of  $\sigma \in K_r^A$  is a point  $z \in \bigcap_{p \in \sigma} V_p \neq \emptyset$  and  $d_\infty(z, p) = \max_{p, q \in \sigma} \frac{d_\infty(p, q)}{2}$  for each  $p \in \sigma$ .

**Proposition A.3.** *Let  $S$  be a finite set of points in  $(\mathbb{R}^d, d_\infty)$ . Given a subset  $e = \{p, q\} \subseteq S$ , we define  $A_e^\bar{r} = \partial \overline{B_{\bar{r}}(p)} \cap \partial \overline{B_{\bar{r}}(q)}$ , where  $\bar{r} = \frac{d_\infty(p, q)}{2}$ . We have that  $A_\sigma^\bar{r} = \overline{B_{\bar{r}}(p)} \cap \overline{B_{\bar{r}}(q)}$  is a non-empty box. Moreover, the set of witness points of  $e$  is  $\mathcal{Z}_e = A_e^\bar{r} \setminus \left(\bigcup_{y \in S \setminus e} \overline{B_{\bar{r}}(y)}\right)$ , and  $e$  belongs to the  $\ell_\infty$ -Delaunay complex of  $S$  if and only if  $\mathcal{Z}_e$  is non-empty.*

*Proof.*  $A_e^\bar{r}$  is the intersection of the boundaries of the closed balls  $\overline{B_{\bar{r}}(p)}$  and  $\overline{B_{\bar{r}}(q)}$ , which are axis-parallel hypercubes. So we have  $A_e^\bar{r} \subseteq \overline{B_{\bar{r}}(p)} \cap \overline{B_{\bar{r}}(q)}$ , because  $\partial \overline{B_{\bar{r}}(p)} \subseteq \overline{B_{\bar{r}}(p)}$  and  $\partial \overline{B_{\bar{r}}(q)} \subseteq \overline{B_{\bar{r}}(q)}$ . Moreover  $\overline{B_{\bar{r}}(p)} \cap \overline{B_{\bar{r}}(q)} \subseteq \partial \overline{B_{\bar{r}}(p)} \cap \partial \overline{B_{\bar{r}}(q)} = A_e^\bar{r}$ , because we can show a contradiction if  $(\overline{B_{\bar{r}}(p)} \cap \overline{B_{\bar{r}}(q)}) \setminus A_e^\bar{r}$  is non-empty. In particular, given  $y \in (\overline{B_{\bar{r}}(p)} \cap \overline{B_{\bar{r}}(q)}) \setminus A_e^\bar{r}$  we have  $d_\infty(y, p) \leq \bar{r}$  and  $d_\infty(y, q) \leq \bar{r}$ , and at least one of these two distances must be strictly less than  $\bar{r}$ , i.e.  $d_\infty(y, p) < \bar{r}$  or  $d_\infty(y, q) < \bar{r}$ . Applying the triangular inequality to these distances, we obtain  $\bar{r} + \bar{r} > d_\infty(p, y) + d_\infty(y, q) \geq d_\infty(p, q) = 2\bar{r}$ , which is the

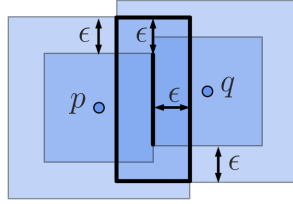


Figure A.11: The  $\varepsilon$ -thickening of the non-empty intersection of two squares equals the intersection of the  $\varepsilon$ -thickenings of the squares.

desired contradiction. Thus  $A_e^{\bar{r}} = \overline{B_{\bar{r}}(p)} \cap \overline{B_{\bar{r}}(q)}$ , which is the Cartesian product of the intervals defining  $\overline{B_{\bar{r}}(p)}$  and  $\overline{B_{\bar{r}}(q)}$ , because Cartesian product and intersections commute, and is non-empty by definition of  $\bar{r}$ . Furthermore

$$\begin{aligned} A_e^{\bar{r}+\varepsilon} &= \overline{\partial B_{\bar{r}+\varepsilon}(p)} \cap \overline{\partial B_{\bar{r}+\varepsilon}(q)} \\ &\subseteq \overline{B_{\bar{r}+\varepsilon}(p)} \cap \overline{B_{\bar{r}+\varepsilon}(q)} \\ &= \varepsilon(\overline{B_{\bar{r}}(p)}) \cap \varepsilon(\overline{B_{\bar{r}}(q)}) = \varepsilon(A_e^{\bar{r}}), \end{aligned}$$

because we can apply Proposition A.1 (ii) with  $\varepsilon(A_e^{\bar{r}}) = \varepsilon(\overline{B_{\bar{r}}(p)} \cap \overline{B_{\bar{r}}(q)})$ . Hence  $A_e^{\bar{r}+\varepsilon} \subseteq \varepsilon(A_e^{\bar{r}})$  for any  $\varepsilon \geq 0$ . With this result we can show the equivalence of  $e$  being a  $\ell_\infty$ -Delaunay edge and  $Z_e$  being non-empty.

( $\Rightarrow$ ) The pair  $e = \{p, q\}$  is a Delaunay edge, so  $V_p \cap V_q \neq \emptyset$ . Equivalently there exist  $\varepsilon \geq 0$  and  $z \in \mathbb{R}^d$  such that  $z \in A_e^{\bar{r}+\varepsilon} \setminus (\bigcup_{y \in S \setminus e} B_{\bar{r}+\varepsilon}(y))$ , where  $\bar{r} = \frac{d_\infty(p, q)}{2}$ .

We prove this direction of the result by contradiction. Let us suppose  $A_e^{\bar{r}}$  is covered by  $\bigcup_{y \in S \setminus e} B_{\bar{r}}(y)$ , i.e.  $Z_e$  is empty. We know that  $A_e^{\bar{r}+\varepsilon} \subseteq \varepsilon(A_e^{\bar{r}})$  from the discussion above, and applying Proposition A.1 (iii) and (iv) we derive the following inclusions

$$A_e^{\bar{r}+\varepsilon} \subseteq \varepsilon\left(A_e^{\bar{r}}\right) \subseteq \varepsilon\left(\bigcup_{y \in S \setminus e} B_{\bar{r}}(y)\right) = \bigcup_{y \in S \setminus e} B_{\bar{r}+\varepsilon}(y),$$

for any  $\varepsilon \geq 0$ . Thus  $A_e^{\bar{r}+\varepsilon} \subseteq \bigcup_{y \in S \setminus e} B_{\bar{r}+\varepsilon}(y)$ , which contradicts the existence of  $z \in A_e^{\bar{r}+\varepsilon} \setminus (\bigcup_{y \in S \setminus e} B_{\bar{r}+\varepsilon}(y))$  for any  $\varepsilon \geq 0$ .

( $\Leftarrow$ ) Any point in  $Z_e \neq \emptyset$  belongs to  $V_p \cap V_q$ , so that  $e \in K^D$ .  $\square$

The above result is illustrated in Figure A.12, which shows how this characterization of Delaunay edges does not hold in Euclidean metric.

**Proposition A.4.** *Let  $S$  be a finite set of points in general position in  $(\mathbb{R}^2, d_\infty)$  and  $r \geq 0$ . Both the Delaunay complex  $K^D$  and the Alpha complex  $K_r^A$  of  $S$  are flag complexes and  $e = \{p, q\} \in K_r^A$  if and only if  $\frac{d_\infty(p, q)}{2} \leq r$ .*

*Proof.* Let us consider three points  $x_1, x_2, x_3 \subseteq S$ , such that  $\{x_1, x_2\}$ ,  $\{x_1, x_3\}$  and  $\{x_2, x_3\}$  are Delaunay edges. Without loss of generality, we can assume  $\{x_1, x_2\}$  to be the longest edge. Defined  $\bar{r} = \frac{d_\infty(x_1, x_2)}{2}$ , and  $A_{x_1 x_2}^{\bar{r}} = \overline{\partial B_{\bar{r}}(x_1)} \cap \overline{\partial B_{\bar{r}}(x_2)}$ , by Proposition A.3 we have that  $A_{x_1 x_2}^{\bar{r}} = \overline{B_{\bar{r}}(x_1)} \cap \overline{B_{\bar{r}}(x_2)}$ , which is a non-empty axis-parallel line segment of length less than  $2\bar{r}$ . Moreover, by definition of  $\bar{r}$ , the intersections  $\overline{B_{\bar{r}}(x_1)} \cap \overline{B_{\bar{r}}(x_2)}$ ,  $\overline{B_{\bar{r}}(x_1)} \cap \overline{B_{\bar{r}}(x_3)}$ , and  $\overline{B_{\bar{r}}(x_2)} \cap \overline{B_{\bar{r}}(x_3)}$  are non-empty, so that by the properties of  $\ell_\infty$ -balls  $A_{x_1 x_2}^{\bar{r}} \cap \overline{B_{\bar{r}}(x_3)}$  is. If  $A_{x_1 x_2}^{\bar{r}} \setminus \overline{B_{\bar{r}}(x_3)} = \emptyset$ , then  $A_{x_1 x_2}^{\bar{r}}$  is covered by  $\overline{B_{\bar{r}}(x_3)}$ , which is in contradiction

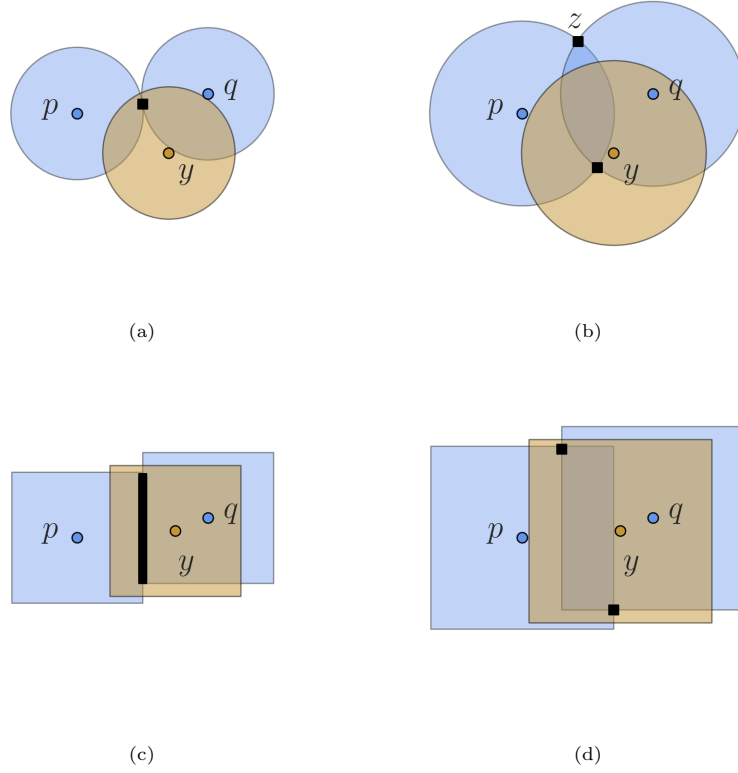


Figure A.12: In (a) Euclidean balls centered in  $p, q$  intersect in a point which is covered by the ball centered in  $y$ . As the radius grows in (b) this intersection is not covered by the ball centered in  $y$ , so that  $z$  is a witness point of  $e = \{p, q\}$ . In (c)  $\ell_\infty$ -balls centered in  $p, q$  intersect in  $A_e^{\bar{r}}$  which is covered by the  $\ell_\infty$ -ball centered in  $y$ . Again the radius grows in (d), but in this case the  $\ell_\infty$ -ball centered in  $y$  covers  $A_e^{\bar{r}+\varepsilon}$ .

with  $\{x_1, x_2\}$  being a Delaunay edge from Proposition A.3. On the other hand, if  $A_{x_1x_2}^{\bar{r}} \setminus \overline{B_{\bar{r}}(x_3)} \neq \emptyset$ , then line segment  $A_{x_1x_2}^{\bar{r}}$  must intersect the boundary of the square  $\overline{B_{\bar{r}}(x_3)}$ . Defined  $\tau = \{x_1, x_2, x_3\}$  and  $A_\tau^{\bar{r}} = A_{x_1x_2}^{\bar{r}} \cap \partial \overline{B_{\bar{r}}(x_3)}$ , we have that the set of witness points of  $\tau$  is  $\mathcal{Z}_\tau = A_\tau^{\bar{r}} \setminus (\bigcup_{y \in S \setminus \tau} \overline{B_{\bar{r}}(y)})$ .

Hence if  $\mathcal{Z}_\tau$  is non-empty, we can conclude that the Delaunay complex of  $S$  is a clique complex from the definition of witness point. We suppose by contradiction that  $\mathcal{Z}_\tau = \emptyset$ , and show that in every possible case one between  $\{x_1, x_2\}$ ,  $\{x_1, x_3\}$ , and  $\{x_2, x_3\}$  cannot be a Delaunay edge.

We know that the axis-parallel square  $\overline{B_{\bar{r}}(x_3)}$  intersects  $A_{x_1x_2}^{\bar{r}}$  without covering it, so that  $A_\tau^{\bar{r}}$  is a point by our general position assumption. To simplify the exposition, we assume without loss of generality  $A_{x_1x_2}^{\bar{r}}$  to be a vertical line segment in  $\mathbb{R}^2$ , and  $\overline{B_{\bar{r}}(x_3)}$  to be intersecting  $A_{x_1x_2}^{\bar{r}}$  from below. More precisely, given  $x_1 = (x_1^1, x_2^1)$ ,  $x_2 = (x_1^2, x_2^2)$ , and  $x_3 = (x_1^3, x_2^3)$ , we assume  $d_\infty(x_1, x_2) = |x_1^1 - x_1^2| = 2\bar{r} \geq |x_1^1 - x_2^1|$ , and that  $x_2^3 \leq \min\{x_2^1, x_2^2\}$ . This implies

$$A_\tau^{\bar{r}} \subseteq A_{x_1x_2}^{\bar{r}} \cap \overline{B_{\bar{r}}(x_3)} = [a_1, a_1] \times [a_2, \hat{b}_2]$$

where  $a_1 = \max\{x_1^1, x_2^1\} - \bar{r}$ ,  $a_2 = \max\{x_2^1, x_2^2\} - \bar{r}$ ,  $b_2 = \min\{x_2^1, x_2^2\} + \bar{r}$ , and  $\hat{b}_2 = x_2^3 + \bar{r}$ . So  $A_\tau^{\bar{r}} = (a_1, \hat{b}_2)$ , and because we are assuming by contradiction that  $A_\tau^{\bar{r}}$  is covered by balls of radius  $\bar{r}$  centered in the points of  $S \setminus \tau$ , there exists  $y' \in S \setminus \tau$  such that  $(a_1, \hat{b}_2) \in \overline{B_{\bar{r}}(y')}$ . Finally, either  $\overline{B_{\bar{r}}(y')}$  intersects  $A_{x_1x_2}^{\bar{r}}$  from above or from below. These two cases are illustrated in Figures A.13a and A.13b, where the boundary of  $\overline{B_{\bar{r}}(y')}$  is represented as a dashed line, and  $A_\tau^{\bar{r}} = (a_1, \hat{b}_2)$  as a red square marker. In the former case  $\overline{B_{\bar{r}}(x_3)} \cup \overline{B_{\bar{r}}(y')}$  covers  $A_{x_1x_2}^{\bar{r}}$ , which is in contradiction with  $\{x_1, x_2\}$  being a Delaunay edge, by Proposition A.3. In the latter

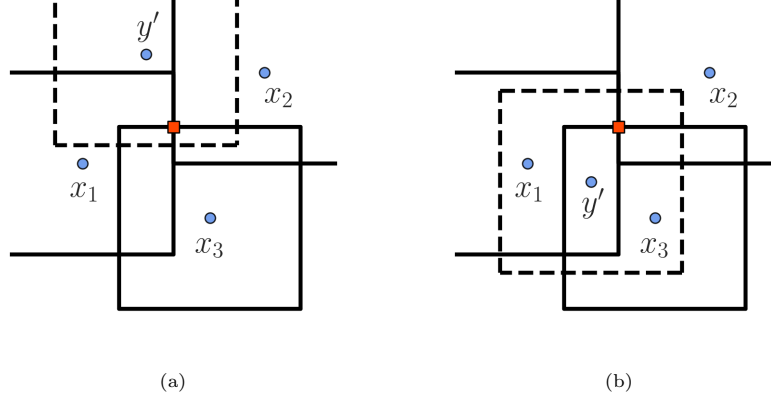


Figure A.13: Illustration of the last two cases of the proof of Proposition ???. In (a) the red square marker represents point  $(a_1, \hat{b}_2)$  on  $A_{x_1 x_2}^{\bar{r}}$ , which is covered by  $B_{\bar{r}}(y')$  from above. In (b) the same point is covered by  $B_{\bar{r}}(y')$  from below. In both (a) and (b) the boundary of  $B_{\bar{r}}(y')$  is drawn as a dashed line.

case, given  $y' = (y^1, y^2)$ , we have  $\min\{x_1^1, x_2^1\} < y^1 < \max\{x_1^1, x_2^1\}$ , and  $x_3^2 < y^2 < \min\{x_1^2, x_2^2\}$ , because  $\overline{B_{\bar{r}}(y')}$  intersects  $A_{x_1 x_2}^{\bar{r}}$  without covering it, and contains  $(a_1, \hat{b}_2)$ . As a result  $y'$  is either in  $\text{Mini}_{x_1 x_3}$  or  $\text{Mini}_{x_2 x_3}$ , depending on  $y^1$  being on the right or left of  $x_3^1$ , and either  $\{x_1, x_3\}$  or  $\{x_2, x_3\}$  is a non-Delaunay edge by Proposition 5.2, which again is a contradiction. Thus  $K^D$  is a flag complex.

We conclude by showing that  $K_r^A$  is also a flag complex. By Proposition A.3 any edge  $e = \{p, q\}$  is added into  $K_r^A$  at  $r = \frac{d_{\infty}(p, q)}{2}$ . Moreover, when the longest edge of any Delaunay triangle  $\tau$  is added at radius  $\bar{r}$ , also  $\tau$  is added in  $K_{\bar{r}}^A$ , because from the discussion above there exist a point  $A_{\bar{r}}^{\bar{r}}$  at distance  $\bar{r}$  from the vertices of  $\tau$ , which is a witness of this triangle.  $\square$

## B. Supporting Results for Proof of Alpha Flag and Čech Equivalence

In this section we present results used in the proof of Theorem 4.3.

**Proposition B.1.** *Let  $B_1$  and  $B_2$  be two boxes in  $\mathbb{R}^d$ . If  $B_1 \cap B_2$  is non-empty, then the Euclidean projection  $\pi_{B_1} : B_1 \rightarrow B_2$ , defined by mapping each  $x \in B_1$  to its closest points in Euclidean distance on  $B_2$ , is such that  $\pi_{B_1}(B_1) \subseteq B_1 \cap B_2$ .*

*Proof.* Let  $B_1 = \prod_{i=1}^d [a_i^{B_1}, b_i^{B_1}]$  and  $B_2 = \prod_{i=1}^d [a_i^{B_2}, b_i^{B_2}]$  such that  $B_1 \cap B_2 \neq \emptyset$ . Because Cartesian products and intersections of intervals commute, we have that  $[a_i^{B_1}, b_i^{B_1}] \cap [a_i^{B_2}, b_i^{B_2}] = [\bar{a}_i, \bar{b}_i] \neq \emptyset$  for each  $1 \leq i \leq d$ , and  $B_1 \cap B_2 = \prod_{i=1}^d [\bar{a}_i, \bar{b}_i]$ .

Given  $x \in B_1$ , we suppose by contradiction that  $y = \pi_{B_1}(x) \in B_2$  is such that  $y \notin B_1 \cap B_2$ . Thus  $y \notin \prod_{i=1}^d [\bar{a}_i, \bar{b}_i]$ , and there exists  $1 \leq \hat{i} \leq d$  such that  $y_{\hat{i}} \notin [\bar{a}_{\hat{i}}, \bar{b}_{\hat{i}}]$ . The intervals  $[a_{\hat{i}}^{B_1}, b_{\hat{i}}^{B_1}]$  and  $[a_{\hat{i}}^{B_2}, b_{\hat{i}}^{B_2}]$  can intersect in four possible ways:

- (i)  $[a_{\hat{i}}^{B_1}, b_{\hat{i}}^{B_1}]$  intersects  $[a_{\hat{i}}^{B_2}, b_{\hat{i}}^{B_2}]$  on the left, i.e.  $a_{\hat{i}}^{B_1} \leq a_{\hat{i}}^{B_2} \leq b_{\hat{i}}^{B_1} \leq b_{\hat{i}}^{B_2}$ . Thus  $a_{\hat{i}}^{B_1} \leq x_{\hat{i}} \leq b_{\hat{i}}^{B_1} < y_{\hat{i}}$ , and we define  $y' = [y_1, \dots, b_{\hat{i}}^{B_1}, \dots, y_d]$ ;
- (ii)  $[a_{\hat{i}}^{B_1}, b_{\hat{i}}^{B_1}]$  intersects  $[a_{\hat{i}}^{B_2}, b_{\hat{i}}^{B_2}]$  on the right, i.e.  $a_{\hat{i}}^{B_2} \leq a_{\hat{i}}^{B_1} \leq b_{\hat{i}}^{B_2} \leq b_{\hat{i}}^{B_1}$ . Thus  $y_{\hat{i}} < a_{\hat{i}}^{B_1} \leq x_{\hat{i}} \leq b_{\hat{i}}^{B_1}$ , and we define  $y'' = [y_1, \dots, a_{\hat{i}}^{B_1}, \dots, y_d]$ ;
- (iii)  $[a_{\hat{i}}^{B_1}, b_{\hat{i}}^{B_1}]$  is contained in  $[a_{\hat{i}}^{B_2}, b_{\hat{i}}^{B_2}]$ , i.e.  $a_{\hat{i}}^{B_2} \leq a_{\hat{i}}^{B_1} \leq b_{\hat{i}}^{B_1} \leq b_{\hat{i}}^{B_2}$ . Thus  $a_{\hat{i}}^{B_1} \leq x_{\hat{i}} \leq b_{\hat{i}}^{B_1} < y_{\hat{i}}$  or  $y_{\hat{i}} < a_{\hat{i}}^{B_1} \leq x_{\hat{i}} \leq b_{\hat{i}}^{B_1}$ , and in the first case we define  $y' = [y_1, \dots, b_{\hat{i}}^{B_1}, \dots, y_d]$  and in the second  $y'' = [y_1, \dots, a_{\hat{i}}^{B_1}, \dots, y_d]$ ;

(iv)  $[a_i^{B_1}, b_i^{B_1}]$  contains  $[a_i^{B_2}, b_i^{B_2}]$ , i.e.  $a_i^{B_1} \leq a_i^{B_2} \leq b_i^{B_2} \leq b_i^{B_1}$ .

In case (iv) we have a contradiction as

$$y_i \in [a_i^{B_2}, b_i^{B_2}] = [\bar{a}_i, \bar{b}_i] \not\equiv y_i.$$

In the other three cases, taken either  $y'$  or  $y''$  we have

$$d_2(x, y') = \sqrt{(x_i - b_i^{B_1})^2 + \sum_{i=1, i \neq \hat{i}}^d (x_i - y_i)^2} < \sqrt{\sum_{i=1}^d (x_i - y_i)^2} = d_2(x, y), \quad (\text{B.1})$$

$$d_2(x, y'') = \sqrt{(x_i - a_i^{B_1})^2 + \sum_{i=1, i \neq \hat{i}}^d (x_i - y_i)^2} < \sqrt{\sum_{i=1}^d (x_i - y_i)^2} = d_2(x, y). \quad (\text{B.2})$$

because  $(x_i - b_i^{B_1})^2 < (x_i - y_i)^2$  in Equation (B.1), and  $(x_i - a_i^{B_1})^2 < (x_i - y_i)^2$  in Equation (B.2). The proof follows because this contradicts  $y$  being the closest point in Euclidean distance to  $x$  in  $B_2$ .  $\square$

**Proposition B.2.** *Let  $S$  be a finite set of points in  $(\mathbb{R}^d, d_\infty)$ . Given  $e = \{p, q\} \subseteq S$ , we have that  $\text{Nrv}(\{\overline{B_{\bar{r}}(y)}\}_{y \in \bar{\mathcal{Y}}})$  has the homotopy type of  $A_e^{\bar{r}}$ , where  $\bar{r} = \frac{d_\infty(p, q)}{2}$  and  $\bar{\mathcal{Y}} = \{y \in S \mid d_\infty(y, p) < 2\bar{r} \text{ and } d_\infty(y, q) < 2\bar{r}\}$ .*

*Proof.* From the Nerve Theorem 3.1 it follows that  $\text{Nrv}(\{\overline{B_{\bar{r}}(y)}\}_{y \in \bar{\mathcal{Y}}})$  and  $\bigcup_{y \in \bar{\mathcal{Y}}} \overline{B_{\bar{r}}(y)}$  are homotopy equivalent, because convex sets are contractible. We show how to define a deformation retraction

$$\phi : \left( \bigcup_{y \in \bar{\mathcal{Y}}} \overline{B_{\bar{r}}(y)} \right) \times [0, 1] \rightarrow A_e^{\bar{r}}.$$

Given  $\phi$ , we have that the sets  $\bigcup_{y \in \bar{\mathcal{Y}}} \overline{B_{\bar{r}}(y)}$  has the homotopy type of  $A_e^{\bar{r}}$ , which is contractible by its convexity. To obtain  $\phi$ , we first define  $\phi_y : \overline{B_{\bar{r}}(y)} \times [0, 1] \rightarrow A_e^{\bar{r}}$  for each  $y \in \bar{\mathcal{Y}}$ . Given the Euclidean projection  $\pi_{\overline{B_{\bar{r}}(y)}} : \overline{B_{\bar{r}}(y)} \rightarrow A_e^{\bar{r}}$ , we set

$$\phi_y(x, t) = (1 - t) \cdot x + t \cdot \pi_{\overline{B_{\bar{r}}(y)}}(x),$$

for every  $x \in \overline{B_{\bar{r}}(y)}$  and  $t \in [0, 1]$ . From Proposition B.1 we have  $\pi_{\overline{B_{\bar{r}}(y)}}(x) \in \overline{B_{\bar{r}}(y)} \cap A_e^{\bar{r}}$ , so that the straight line segment from  $x$  to  $\pi_{\overline{B_{\bar{r}}(y)}}(x)$  is fully contained in  $\overline{B_{\bar{r}}(y)}$ , by the convexity of this set. Thus  $\phi_y$  is well-defined and continuous by the continuity of  $\pi_{\overline{B_{\bar{r}}(y)}}$ . Then we set

$$\phi(x, t) = \phi_{\hat{y}}(x, t),$$

for every  $x \in \bigcup_{y \in \bar{\mathcal{Y}}} \overline{B_{\bar{r}}(y)}$  and  $t \in [0, 1]$ , with  $\hat{y} \in \bar{\mathcal{Y}}$  such that  $x \in \overline{B_{\bar{r}}(\hat{y})}$ . This might not be well-defined, because for a given  $x$  all the  $\phi_{\hat{y}}$  corresponding to a point in  $\bar{\mathcal{Y}}^x = \{\hat{y} \in \bar{\mathcal{Y}} \mid x \in \overline{B_{\bar{r}}(\hat{y})}\}$  can be used to define  $\phi(x, t)$  for any  $t \in [0, 1]$ . Luckily, given  $R = \bigcap_{\hat{y} \in \bar{\mathcal{Y}}^x} \overline{B_{\bar{r}}(\hat{y})}$ , which is a box containing  $x$ , Proposition B.1 guarantees that  $\pi_R : R \rightarrow A_e^{\bar{r}}$  is such that  $\pi_R(R) \subseteq R \cap A_e^{\bar{r}}$ . Thus  $\phi$  is well-defined because the straight line segment defined by  $(1 - t) \cdot x + t \cdot \pi_R(x)$  for  $t \in [0, 1]$  is contained within  $R$ , again by convexity. Furthermore,  $\phi$  is continuous by the continuity of the Euclidean projections  $\pi_{\overline{B_{\bar{r}}(y)}}$ , and is a deformation retraction onto  $A_e^{\bar{r}}$  because  $A_e^{\bar{r}} \subseteq \bigcup_{y \in \bar{\mathcal{Y}}} \overline{B_{\bar{r}}(y)}$ .  $\square$

**Proposition B.3.** *Let  $K_1$  and  $K_2$  be two abstract simplicial complexes such that  $K_1 \subseteq K_2$ . If there is only one edge  $e$  contained in  $K_2$  and not in  $K_1$ , and it exists a triangle  $\tau \in K_2$  of which  $e$  is a face, then  $H_1(K_2)$  cannot contain an homology class  $[\gamma]$  not in  $H_1(K_1)$ .*

*Proof.* Any 1-cycle representing an homology class  $[\gamma]$  such that  $[\gamma] \in H_1(K_2)$  and  $[\gamma] \notin H_1(K_1)$  must contain  $e$ . But given  $e = \{p, q\}$  and  $\tau = \{p, q, y\}$ , any such 1-cycle would be homologous to a formal sum containing  $\{p, y\}$  and  $\{y, q\}$  in place of  $e$ . Thus it would exist a 1-cycle representing  $[\gamma]$  containing edges in  $K_1$  only, which is in contradiction with  $[\gamma] \notin H_1(K_1)$ .  $\square$



## C. Notation

### Preliminaries

- $\text{St}(\tau)$  star of  $\tau \subseteq K$ ,  $\text{Lk}(\tau)$  link of  $\tau \subseteq K$ .
- $B_r(p)$  open ball,  $\overline{B_r(p)}$  closed ball,  $\partial\overline{B_r(p)}$  boundary of closed ball.
- $V_p$  Voronoi region,  $K^D$  Delaunay complex.

### Persistent Homology

- $K_{\mathcal{R}}$  filtration of  $K$  parameterized by  $\mathcal{R} = \{r_i\}_{i=1}^m$ .
- $M_k(K_{\mathcal{R}})$  is the  $k$ -th persistence module of  $K_{\mathcal{R}}$ .
- $d_B(\text{Dgm}_k(K^1), \text{Dgm}_k(K^2))$  is the bottleneck distance.
- $K_{\mathcal{R}}^{VR}$  VR filtration,  $K_{\mathcal{R}}^{\check{C}}$  Čech filtration,  $K_{\mathcal{R}}^A$  Alpha filtration.

### Delaunay Edges

- Given  $\sigma \subseteq S$ ,  $\bar{r} = \frac{\max_{p,q \in \sigma} d_{\infty}(p,q)}{2}$ .
- $z$  is witness of  $\sigma$  if  $z \in \bigcap_{p \in \sigma} V_p \neq \emptyset$  and  $d_{\infty}(z, p) = \bar{r}$  for each  $p \in \sigma$ .
- $A_e^{\bar{r}+\varepsilon} = \bigcap_{p \in \sigma} \partial\overline{B_{\bar{r}+\varepsilon}(p)}$  for  $\varepsilon \geq 0$ .
- Given an edge  $e = \{p, q\}$ ,  $A_e^{\bar{r}} = \partial\overline{B_{\bar{r}}(p)} \cap \partial\overline{B_{\bar{r}}(q)} = \overline{B_{\bar{r}}(p)} \cap \overline{B_{\bar{r}}(q)}$  is a non-empty box. If a witness of  $e = \{p, q\}$  exists, then it must belong to  $A_e^{\bar{r}}$ .

### Alpha Clique and Minibox Complexes

- $\text{Mini}_{pq} = \prod_{i=1}^d (\min\{p_i, q_i\}, \max\{p_i, q_i\})$ .
- $K_{\mathcal{R}}^{AF}$  Alpha flag filtration,  $K_{\mathcal{R}}^M$  Minibox filtration.